Xenosialitis modulates the function of the Alzheimer's disease associated SIGLEC3 in human THP1 macrophages

Dissertation

zur
Erlangung des Doktorgrades (Dr. rer. nat.)
der
Mathematisch-Naturwissenschaftlichen Fakultät
der
Rheinischen Friedrich-Wilhelms-Universität Bonn

vorgelegt von

Mona Ann Mathews

aus

Chennai, Indien

Bonn, November 2016

Angefertigt mit Genehmigung der Mathematisch-Naturwissenschaftlichen Fakultät
der Rheinischen Friedrich-Wilhelms-Universität Bonn

1. Gutachter: Prof. Dr. Harald Neumann
2. Gutachter: Prof. Dr. Walter Witke

Tag der Promotion: 10.04.2017

Erscheinungsjahr: 2018

Contents

Abbreviations

Aβ	Amyloid-β
AD	Alzheimer's disease
ALS	Amyotrophic lateral sclerosis
APOE	Apolipoprotein E
BDNF	Brain derived neurotrophic factor
BSA	Bovine serum albumin
nbAβ	non-biotinylated Aβ
CD	Cluster of differentiation
cDNA	Complementary Deoxyribonucleic acid
CNS	Central nervous system
CR1	complement receptor 1
CR3	complement receptor 3
Cy	Cyanine
DAPI	4',6-diamidino-2-phenylindole
DMSO	Dimethyl sulfoxide
dNTP	deoxyribonucleotide
EBs	Embryoid bodies
EDTA	Ethylenediaminetetraacetic acid
FCS	Fetal calf serum
FGF	Fibroblast growth factor
Fn	Fibronectin
GAPDH	Glyceraldehyde 3-phosphate dehydrogenase
GDNF	Glial cell-line derived neurotrophic factors
GM-CSF	Granulocyte-macrophage colony stimulating factor
GWAS	Genome wide association study

IBA-1	Ionized calcium binding adaptor molecule 1
Ig	Immunoglobulin
IgC2	Immunoglobulin C2-type
IgV	Immunoglobulin V-like
IFN	Interferon
IL	Interleukin
iPS cells	Induced pluripotent stem cells
iPSdM	Induced pluripotent stem cell derived microglia
ITAM	Immunoreceptor tyrosine-based activation motif
ITIM	Immunoreceptor tyrosine-based inhibitory motif
KO/SR	Knockout serum replacement
LOAD	Late onset Alzheimer’s disease
LPS	Lipopolysaccharide
Lm	Laminin
M-CSF	Macrophage colony stimulating factor
MEF	Murine embryonic fibroblasts
NEAA	Non-essential amino acids
Neu5Ac	Acetylated neuraminic/sialic acid
Neu5Gc	Glycosylated neuraminic/sialic acid
NGS	Normal goat serum
NO	Nitric oxide
PBS	Phosphate Buffer Solution
PCR	Polymerase chain reaction
PE	Phycoerythrin
PFA	Paraformaldehyde
PLL	Poly-L-Lysine
PLO	Poly-L-Ornithine

PMA	Phorbol 12-myristate 13-acetate
PNS	Peripheral nervous system
Rh	Recombinant human
RNA	Ribonucleic acid
ROS	Reactive oxygen species
RT	Reverse transcription
SHP	Src homology region 2 domain-containing phosphatase
SIGLECs	Sialic acid binding Ig-like lectins
T_A	Annealing temperature
TBE	Tris/Borate/EDTA
TGF	Transforming growth factor
TLR	Toll-like receptor
TNF	Tumor necrosis factor
WT	Wildtype

1. Introduction

Humans enjoy a unique dominance over plants and animals. This dominance advanced with the development of a complex and adaptive central nervous system (CNS). CNS, comprising of the brain and spinal cord, is vital for integration and processing of information to achieve coordinated functioning of an organism. The human brain is a complex organ made up of two major cells types; neurons and glia. Neurons are considered to be the building blocks of the CNS and therefore degeneration of neurons leads to gross impairment. A physiological state would require homeostasis of the 10^{11} neuronal cells regulated by upto 10-50 times more numbers of glial cells, followed by cooperative functioning between nervous systems and motor coordination. However, several factors could lead to degeneration of neurons. Neurodegeneration can be caused by external factors such as trauma and pathogens or internal factors such as misfolded proteins, genetic mutations or inappropriate functioning of supportive cells in the CNS - such as microglia, astrocytes or oligodendrocytes. Microglia in particular have already been implicated as key players in brain injury as well as disease by several researchers (reviewed by Kreutzberg 1996)(Kettenmann et al. 2011) Understanding the factors involved in neurodegeneration on a cellular level is necessary to develop successful therapies against neurodegenerative diseases.

1.1 Microglia: characteristics and functions

Microglia, the smallest of the glial cells, are distributed in the brain and spinal cord and account for 20 % of the total population of glial cells in the CNS (Kreutzberg 1996). The origin of microglia has been recently confirmed by the group led of Florent Ginhoux (Ginhoux et al. 2010) who conducted fate mapping studies in mice. Ginhoux and colleagues proved that adult mouse microglia develop from yolk-sac derived primitive myeloid progenitors that arise before embryonic day 8, during the first wave of hematopoiesis (figure 1, top). These microglial precursors then invade the entire CNS, setting up connections with other neural and glial cells (Ransohoff & Cardona 2010). Following microglial invasion of the CNS, the blood brain barrier develops, leading to the isolation of microglia exclusively in the CNS. Subsequent to this event, peripheral nervous immune cells develop. Therefore there are regional as well as temporal distinctions between microglia and their counterparts in the peripheral

nervous system (PNS). The immune cells of the PNS include among others, monocytes and macrophages. These cell types arise from the second wave of hematopoiesis, namely - the definitive hematopoiesis (figure 1, bottom).

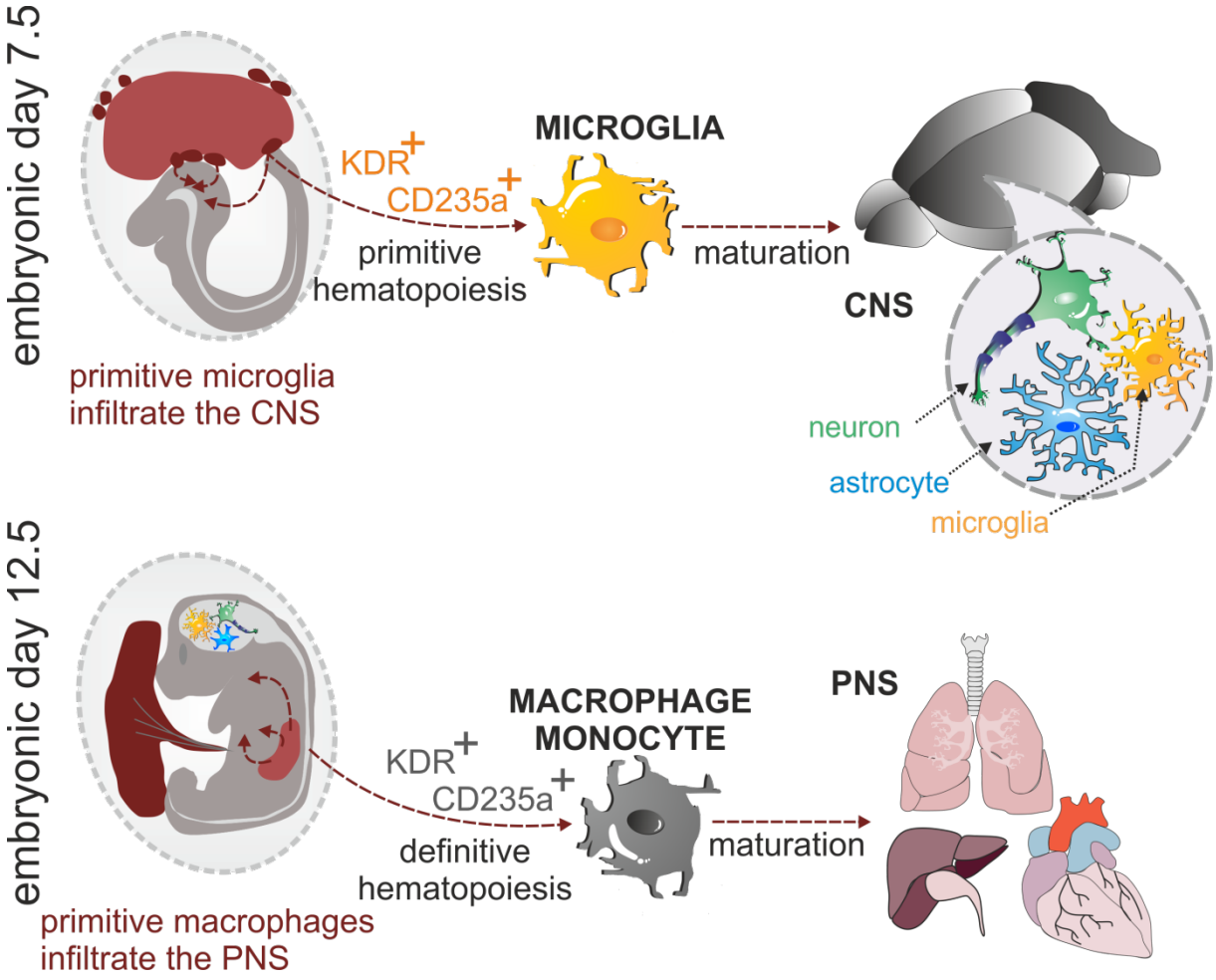

Figure 1: Origins of microglia and macrophages. Microglial cells develop during the first wave of hematopoiesis (primitive) around embryonic day 7.5, in mice. The primitive microglia invade the CNS prior to formation of blood-brain barrier. After which, they mature into the final cell type in the company of neural cell types (top). Macrophages and monocytes develop during the second wave of hematopoiesis (definitive) around embryonic day 12.5, in mice. These cells represent the first immune effector cells of the PNS (bottom).

Therefore, microglia are considered to be the only *resident* immune cells of the CNS, while peripheral immune cells are visitors that may temporarily support microglia in immune responses during pathogenesis. While microglial and their peripheral counterparts partially differ in their origins, the final cell types are rather indistinguishable. Both microglia and macrophages are immune reactive cells which express a comparable array of receptors and functional characteristics. Under

physiological conditions microglia actively survey the CNS to maintain homeostasis (Nimmerjahn et al. 2005). Other physiological functions include synaptic pruning during development and extracellular signaling via cytokines and chemokines to contact other cell types in the CNS which help maintain homeostasis (Tremblay et al. 2010). Therefore, microglia are involved in many aspects of brain functioning and are required to maintain a healthy environment for neuronal signaling. During development microglia are directed by chemical cues to trim excess neuronal synapses in order to fine tune connections in the CNS. After development, when stimulated by chemo- or cytokines from apoptotic cells, microglia phagocytose debris and maintain homeostasis. Besides physiological functions, these cells play a defensive role in immune-compromised conditions such as infectious attack or trauma to the CNS (Kreutzberg 1996). Therefore, they are regarded to be immune effector cells of the CNS.

Microglial immune responses can follow contradictory pathways depending on the type of stimuli they receive (figure 2). During development and homeostasis, microglia are most often stimulated by anti-inflammatory factors, which direct the microglia to follow a neuroprotective pathway through an arginase-dependent metabolism in which arginine leads to tissue repair. On the other hand, when stimulated by lipopolysaccharides (LPS) from invading gram-negative bacteria or by other pro-inflammatory factors, microglia follow a pro-inflammatory pathway which includes production of reactive oxygen species (ROS) (Bosurgi et al. 2011). Acute inflammation is necessary for removal of invading pathogens but also causes collateral damage to neighboring healthy cells. Furthermore, chronically persistent inflammation causes gross degeneration which can gradually spread throughout the CNS.

Due to its importance in maintaining homeostasis in the CNS, pathological developments caused by intrinsic factors often include microglial dysfunction. Malfunctioning microglia are associated with many neurodegenerative diseases such as Alzheimer’s disease (AD), Parkinson’s and Huntington’s disease. Although the specific cause or effects regarding microglia in neurodegenerative diseases are not clearly understood, the capacity of microglia to exhibit both pro- and anti-inflammatory properties (Mclaurin & Ransohoff 2010) are hypothesized to unintentionally support disease progression.

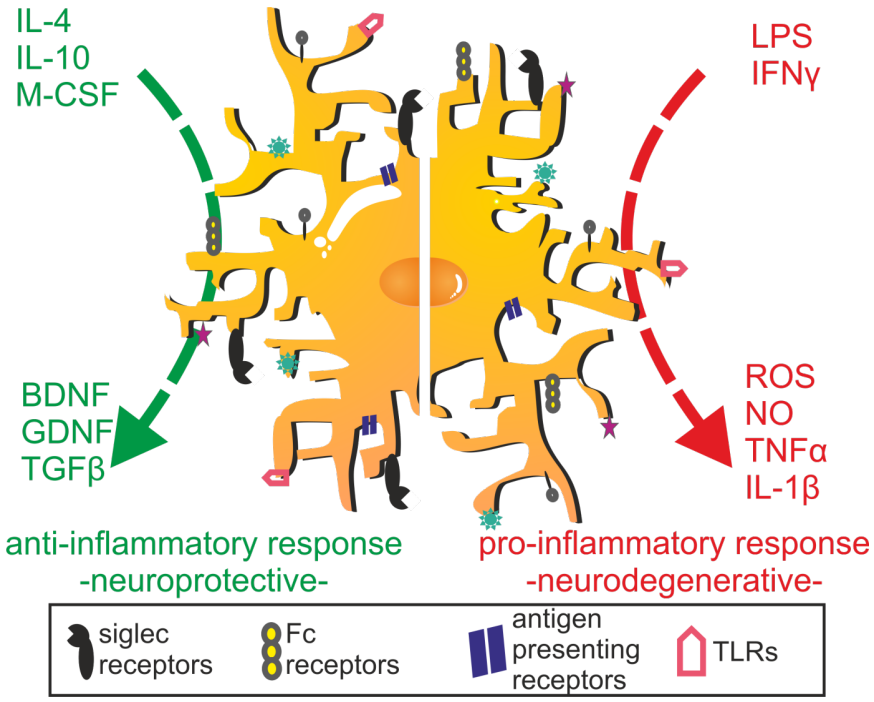

Figure 2: Contrasting microglial responses. The immune response elicited by microglial cells depends on the type of stimuli they receive. Stimuli from anti-inflammatory factors elicit a neuroprotective response (left) with the production of neurotrophic growth factors such as BDNF and GDNF. While stimuli from invading bacteria and other pathogens elicit a pro-inflammatory response (right) characterized by the production of radicals and pro-inflammatory cytokines. BDNF - brain derived neurotrophic factor; GDNF - glial cell line derived neurotrophic factor; IFN - interferon; IL - interleukin; LPS - lipopolysaccharide; M-CSF - macrophage colony stimulating factor; NO - nitric oxide; ROS - reactive oxygen species; SIGLEC - sialic acid binding immunoglobulin-like lectin; TGF - transforming growth factor; TLR - toll like receptor; TNF - tumor necrosis factor.

1.2 Microglia in AD

Microglial cells are a major source for radical and pro-inflammatory cytokine production in the CNS, which could lead to neuroinflammation. Since inflammation is a critical feature of AD, the contribution of microglia to AD onset and progression is in the focus of AD research (Heppner et al. 2015). AD brains develop widespread cortical atrophy leading to cognitive disabilities and memory loss. Pathological features include presence of amyloid plaques and neurofibrillary tangles. The former are dense, insoluble deposits of amyloid-β (Aβ) peptides accumulated in the extracellular space, while the latter refers to aggregates of microtubule-associated protein tau which are hyperphosphorylated and accumulate intracellularly in neurons (figure 3).

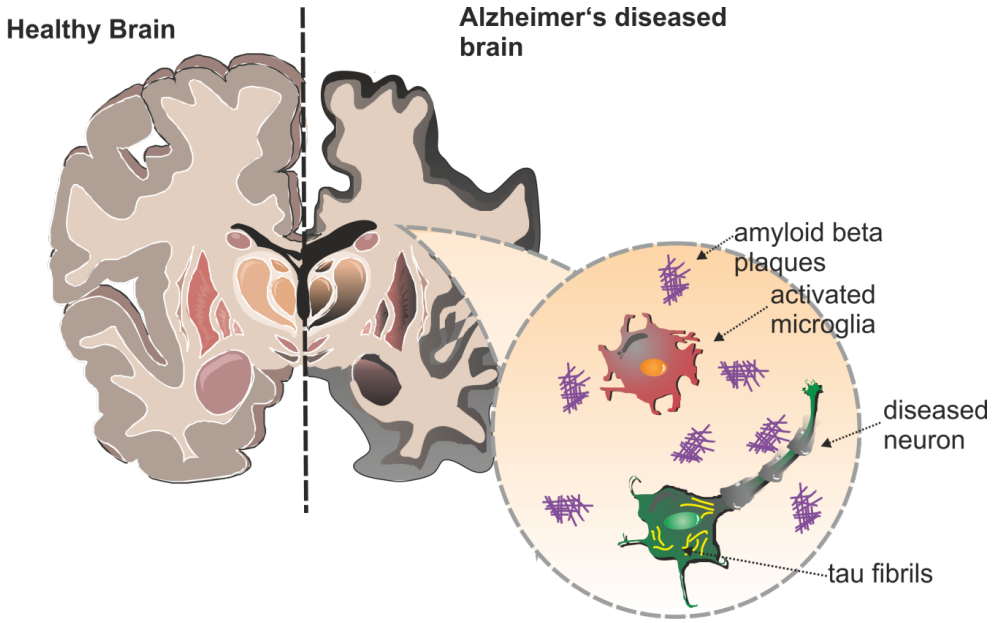

Figure 3: Pathological features of Alzheimer's disease (AD) brain. In comparison to a healthy non-demented brain (left), the brain of an AD patient (right) shows clear atrophy and shrunken grey matter. On a microscopic level, plaques of Amyloid beta (Aβ) and hyperphosphorylated tau fibrils can be found extracellularly and intracellularly in neurons, respectively. Image of healthy brain was obtained from *Servier powerpoint Image Bank*.

In general, microglia seem to play an ambivalent role in AD brains. On the one hand, they express receptors like Cluster of Differentiation (CD) 14 and toll-like receptors 2 and 4 (TLR 2 and TLR 4) which should support clearance of Aβ plaques (Linnartz et al. 2010). Overall, studies show an increase in reactive microglia specifically localized around amyloid plaques in AD brains (Solito & Sastre 2012). In fact, a correlation between increased microglial reactivity with hightened amyloid load and cognitive impairment has been established (Edison et al. 2008). However, on the other hand, Aβ plaques increasingly accumulate and do not effectively get phagocytosed by the reactive microglia and therefore exacerbate disease progression.

Hellwig and colleagues clearly showed that accumulation and formation of amyloid plaques occurred more readily in organotypic hippocampal slices depleted of microglia (Hellwig et al. 2015). Since microglial ablation leads to increased plaque formation, it can be concluded that microglia are vital in keeping Aβ plaques in check. This conclusion was further confirmed when they showed that replenishing the microglial-ablated organotypic cultures with microglia from wildtype (WT) mice reversed plaque formation. Most interestingly, when the microglial-ablated organotypic cultures were replenished with microglia from an AD model mouse, the

Aβ plaques formation was once again increased (Hellwig et al. 2015). These results suggest that the functional capabilities of microglia in an AD model are diminished possibly due to chronic reactivity to fibrillary Aβ. While healthy microglia as well as microglia in the early stages of amyloid formation are still capable of phagocytosing the plaques, microglia chronically exposed to the ever increasing plaque load lose their ability to effectively phagocytose Aβ plaques.

In addition to faulty phagocytosis of Aβ by microglial cells, radical production by microglia has also been described as a feature of AD (Perry 2002, Ansari et al., 2010 and Zhang et al., 2013). Studies on post-mortem AD brains as well as AD mouse models describe increased radical production in comparison to healthy controls. Although, the full contribution of radical damage towards neurodegeneration with respect to AD was initially controversial, studies now describe neuroinflammation as a constitutive event in AD brains (Solito et al., 2012, Heneka et al., 2015). Neuroinflammation is a result of chronic up regulation of pro-inflammatory factors and radical bursts by reactive astrocytes and microglia. In fact, microgliosis has been identified in AD irrespective of the presence of Aβ plaques (Edison et al. 2008)(Yokokura et al. 2011)(Varnum & Ikezu 2012). Therefore, publications describing radical bursts upon treatment with Aβ must be viewed critically. Studies which claim that Aβ causes neuronal damage due to the induction of pro-inflammation make use of high concentrations of Aβ (Milton et al. 2008)(Parajuli et al. 2013). However, these studies do not appropriately mirror the *in vivo* environment of AD onset since Aβ accumulation is a slow and gradual process.

Furthermore, studies which attribute the onset of AD solely to Aβ accumulation no longer hold relevance in view of the recent discovery of AD risk alleles through genome-wide association studies (GWAS). Late onset AD (LOAD) was previously considered to occur spontaneously, as a consequence of several external factors in combination with aging. In 2010, a new breakthrough in LOAD research was brought about by GWA). GWAS identified associations between polymorphisms of several novel genes with LOAD (Hollingworth et al. 2011)(Naj et al. 2011)(Shi et al. 2012). Among these, of particular interest in this project, is an immune-related gene- sialic-acid binding immunoglobulin-like lectin 3 (SIGLEC3).

1.3 Immune receptors in health and disease

SIGLEC3 encodes a protein expressed on the surface of immune cells and plays a role in the innate immune system. SIGLEC3, also known as CD33, binds sialylated molecules and signals via intracellular immunoreceptor tyrosine-based inhibitory motifs (ITIM). Ligand binding facilitates phosphorylation of the receptors' intracellular tyrosine by Src kinase. Phosphorylated tyrosine serves as a docking site for tyrosine phosphatases such as Src homology region 2 domain-containing phosphatase-1 (SHP-1) which in turn dephosphorylate downstream molecules of the activatory signaling pathway. By this way, SIGLEC3 can modulate the downstream molecules of activation receptors, such as triggering receptor expressed on myeloid cells 2 (TREM2), to gradually dampen activation/inflammation and maintain homeostasis (figure 4) (reviewed in Linnartz-Gerlach et al. 2014).

Therefore, SIGLEC3 modulates cellular activation and serves to fine tune the cellular response to stimuli. SIGLEC3 is primarily expressed on cells of myeloid lineage. Therefore, microglia are the only resident immune cells in the CNS which express this receptor. Taking into account the association between polymorphisms of CD33 and LOAD, the hypothesis of microglial activities contributing to disease progression is gaining interest. While the polymorphism rs3865444C of SIGLEC3 has been associated with increased LOAD risk, the polymorphism rs12459419T has been recently identified to be protective against LOAD onset (Griciuc et al. 2013).

The final gene of interest in this project having polymorphisms associated with AD is *trem2*. TREM2, as the name suggests, is expressed on myeloid type cells such as microglia and macrophages. TREM2 in association with the intracellular activatory receptor DAP12 can mediate phagocytosis of apoptotic neurons without inflammation. GWAS have identified a rare missense mutation in the gene encoding TREM2, called the R47H substitution (Wang et al. 2015)(Colonna & Wang 2016). Recent studies have identified that the R47H mutation reduces the binding ability of TREM2, hindering phagocytosis and therefore perhaps allowing Aβ to accumulate (Wang et al., 2015). APOE has been described to be a ligand of TREM2 which can bind Aβ. However, when the binding affinity of TREM2 to its ligand is compromised, the delivered Aβ cannot be consequently phagocytosed.

All in all, polymorphisms of several genes have been associated with increased LOAD risk. Interestingly, a high number of these genes are transcribed in immune cells. The compromised ability to phagocytose when faced with Aβ plaques seems to be a repeated facet of LOAD risk. Both proteins described above; SIGLEC3 and TREM2 are involved in immune response by modulating phagocytosis. Therefore, an event of Aβ accumulation by the malfunctioning of one or more of these genes is highly possible.

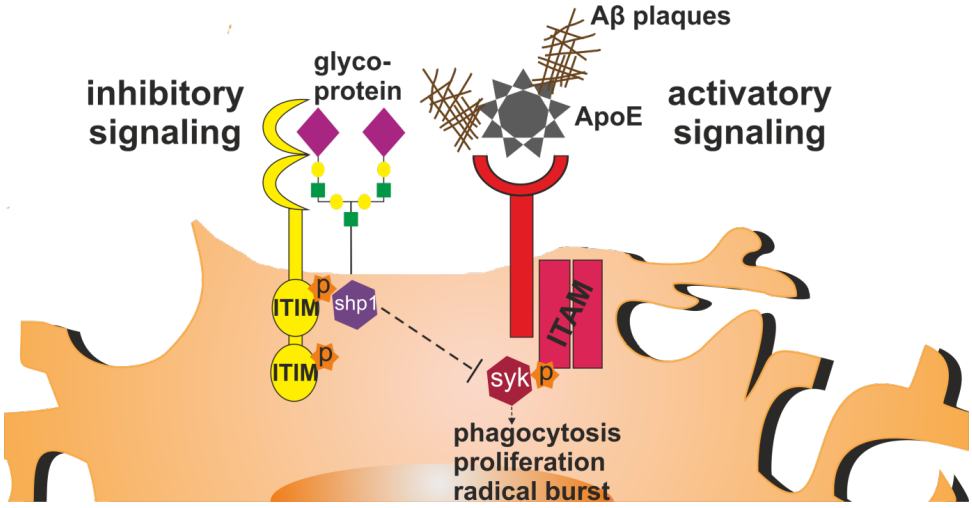

Figure 4: Inhibitory (ITIM) versus activatory (ITAM) signaling. Upon ligand binding to inhibitory receptors, such as certain members of the SIGLEC family, intracellular tyrosine motif gets phosphorylated by tyrosine phosphatases and serves as a docking site for SHP1. As a consequence, the phosphorylated-downstream molecules of the activatory pathway are dephosphorylated and therefore cannot further propagate activation of cellular process, such as phagocytosis and proliferation. ITIM - immunoreceptor tyrosine-based inhibitory motif; ITAM - immunoreceptor tyrosine-based activatory motif; shp - src homology region 2 domain-containing phosphatase 1; p - phosphate; Aβ - amyloid beta; ApoE - apolipoprotein E; TREM2 - triggering receptor expressed on myeloid cells 2; DAP12 - TYRO-protein tyrosine kinase-binding protein 12; syk - spleen tyrosine kinase.

Immune cells, by means of their expressed receptors, are currently in the focus of AD research. Especially malfunctioning receptors that unintentionally propagate disease progression are being extensively researched as putative therapeutic targets, as described above. However, the respective microenvironment that plays a critical role in the maintenance and functioning of all cell types, on a molecular level must not be overlooked. With this in mind, glycobiology - the study of sugars - has been included in this project as a vital theme involved in malfunctioning immune cells with respect to AD development and progression.

1.4 Sialic acids

Previous studies (Samraj et al., 2014, Ma et al., 2016) have already reiterated the influence that different types of sugars or sialic acids have on the functioning of various cell types, including, immune cells. In fact, it is now known that the incorporation of a foreign sialic acid can lead to inflammation called “xenosialitis” (Samraj et al. 2015). Therefore, the fact of developing chronic inflammation, a hallmark of AD, which could be caused by xenosialitis is a topic worth investigating further. To first understand the depths of the influence sugars have on our cells, their molecular and structural characteristics must be studied.

Sialic acids are a family of sugars on a nine-carbon backbone that are primarily found at the ends of glycan chains on the surface of all cell types. N-acetylneuraminic acid (Neu5Ac) is one of the most common and basic forms of sialic acids from which N-glycolylneuraminic acid (Neu5Gc) and other more complicated sialic acids can be derived. Neu5Ac differs from Neu5Gc by a hydroxyl group (figure 5, right). They form glycoproteins or glycol lipids by α-2,3-; α-2,6 or α-2,8 linkages (Varki 2007). Sialic acids play a role in differentiation, growth, cell-cell interactions and signal transduction among other functions (Varki & Gagneux 2012). The highest concentration of sialic acids is found in the brain, where they are present mostly in the form of glycolipids (Collins et al. 1997).

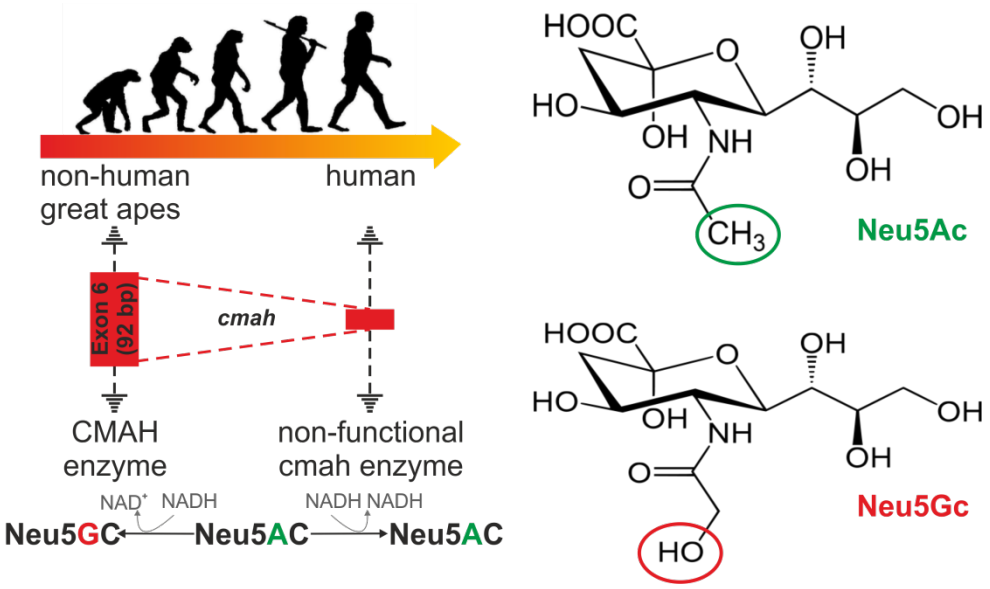

Figure 5: Loss of functional cytidine monophosphate-N-acetylneuraminic acid hydroxylase (CMAH) in humans. During evolution a 96 base pair deletion in gene *cmah*

resulted in humans being the only higher mammals to lack the ability to convert N-acetylneuraminic (Neu5Ac) acid to N-glycolylneuraminic acid (Neu5Gc) (left). NAD^+ / NADH – nicotinamide adenine dinucleotide. Neu5Ac can by hydrolyzed to give rise to Neu5Gc. Therefore the two sialic acids differ by a single oxygen atom (right). Structural images of Neu5Ac and Neu5Gc were modified from *Wikipedia*.

Interestingly, sialic acids are found in the midst of an evolutionary race between vertebrates, which use these sialic acids to fine tune immune responses, and pathogens, which hijack host sialic acids to avoid immune response of the latter (reviewed by Varki 2007). The most notable evolutionary change with regards to sialic acids is the frame shift mutation in the cytidine monophosphate N-acetylneuraminic acid hydroxylase (CMAH) gene caused by a 96-base pair deletion of exon 5 (Padler-Karavani, Hurtado-Ziola, et al. 2013). As a result, Neu5Ac cannot be converted to Neu5Gc (figure 5, left). Therefore, humans experienced a loss of Neu5Gc and accumulation of Neu5Ac and consequently, a change in several receptors which have evolved to recognize these sialic acids. These receptors have evolved to recognize specific types or forms of sialic acids in an attempt to fine tune immune responses (Varki 2010). Therefore, sialic acids that cover most proteins and lipids on the cell surface and their corresponding receptors are emerging as important structures in human physiology. SIGLECS are one such receptor family that is found primarily on the surface of immune cells and oligodendrocytes. The above described SIGLEC3 is a member of the SIGLEC family, with inhibitory signaling capacity in humans.

Humans evolved to not produce Neu5Gc as an attempt to avoid pathogen infiltration using molecular mimicry. However, several studies have shown individuals to have antibodies against Neu5Gc (Padler-Karavani et al., 2013). In fact, Neu5Gc has been found in cancer tissue as well as in embryonic tissue. Naturally, the question arises - Where does this Neu5Gc originate from? Studies by Bardor and colleagues (Bardor et al., 2005) have extensively shown that Neu5Gc can be incorporated from metabolism by micropinocytosis or endocytosis. Since the uptake of the sialic acids occur in a non-receptor mediated manner, both sialic acids are pino-/ endocytosed in a non-biased manner. Neu5Ac and Neu5Gc enter the cell, either as free sialic acids or on glycoproteins. Sialic acids on proteins are first separated by lysosomal sialidases and then placed onto new proteins by sialyltransferases. The newly built glycoproteins are then transported to the cell surface to form a part of the glycocalyx

(figure 6). Once Neu5Ac and Neu5Gc are part of the glycocalyx, they are open for receptor binding (or rather mis-binding) leading to a malfunctioning of receptors that depend on sialic acids as endogenous ligands. The previously described SIGLEC 3 is a member of the family of inhibitory SIGLEC receptors and as explained, binds sialic acid. Therefore, it can be postulated that incorporation of foreign sialic acids may negatively influence the binding and functioning of a sialic acid-binding receptor such as SIGLEC3. Considering correlation between SIGLEC3 and LOAD, by extension, it could be hypothesized that sialic acids may play a role in either LOAD development or progression.

Therefore, this thesis focuses on the all-encompassing idea that incorporated sialic acids may influence the functioning of LOAD associated receptors which in turn may be causative or supportive of the neurodegenerative diseases. With this in mind, the concept followed in this project was to identify the influence of foreign sialic acids (Neu5Gc) in comparison to native sialic acids (Neu5Ac) on several typical aspects of microglia functioning. In order to mimic a pre-clinical AD environment, the cells were additionally exposed to nanomolar concentrations of Aβ. The Aβ concentration for this project was intentionally selected to be upto 10 times lower than described in previous publications (Milton et al. 2008; Parajuli et al. 2013), to serve as part of the cellular environment rather than to be a strong stimulation. Several read outs such as phagocytosis capacity, proliferative and apoptotic rate, reactive oxygen species (ROS) production and many more have been extensively studied. These studies could help identify the underlying cause of chronic inflammation as found in AD.

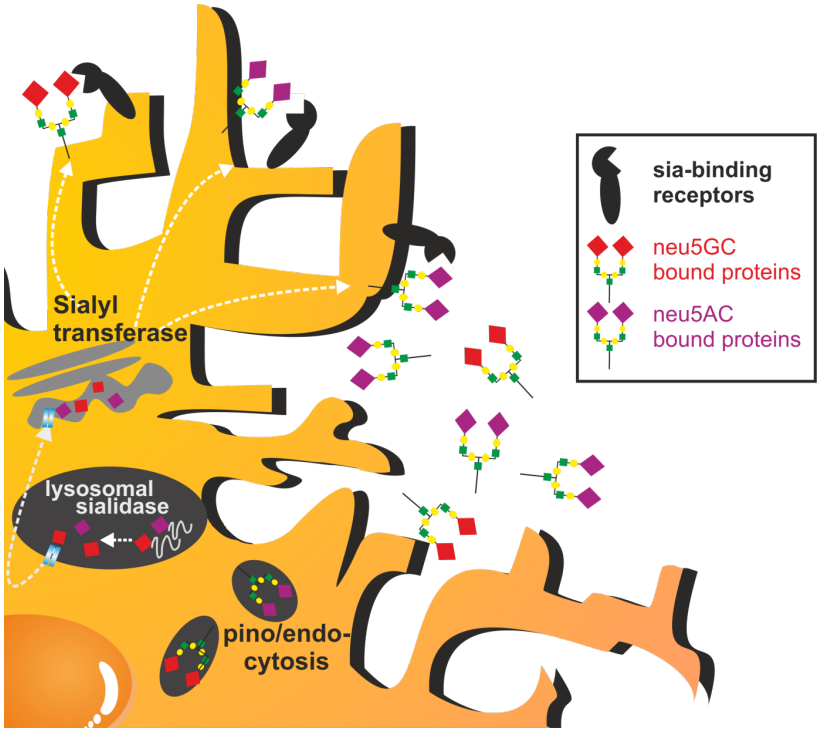

Figure 6: Mechanism of Neu5Gc incorporation. Neu5Gc can be metabolically incorporated in to the cell surface glycocalyx. Neu5Ac as well as Neu5Gc are taken up by pino- or endocytosis, as free sialic acids or in the form of glycoproteins. Once engulfed, the sialic acid-bound glycoprotein is modified by means of lysosomal sialidases and sialyl transferases. The final product is re-introduced on the cell surface glycocalyx, where the sialic acids are exposed and available for receptor binding. Lectin family of receptors such as SIGLECs are capable of binding sialic acids.

1.5 Aim of Study

Chronic inflammation is an undisputed feature of late onset Alzheimer's disease (LOAD). Activated microglia,found around amyloid beta (Aβ) plaques are implicated as the source of inflammation. However they are incapable of efficiently phagocytosing the plaques and therefore lead to Aβ accumulation. The molecular mechanisms responsible for this ambivalent and ultimately neurodestructive behavior of microglia remains elusive. Studies show that the deposition of Aβ occurs in demented as well as non-demented individuals. Therefore, deposition of Aβ is not solely responsible for disease onset nevertheless accumulation of Aβ plaques possibly exacerbates LOAD progression. Furthermore, Genome-wide association studies (GWAS) have identified polymorphisms of several genes, including SIGLEC3 and TREM2 found on microglia, which increase LOAD risk. Both proteins are involved either directly or indirectly with maintenance of homeostasis and phagocytosis. Therefore, it is conceivable that dysregulation of these proteins could cause inflammation and faulty phagocytosis as seen in LAOD patients.

The objective of this project was to establish a human microglial model system to study SIGLEC3 signaling and SIGLEC3 receptor interaction with sialic acids in AD pathology. A human model system is critical since SIGLEC3 is highly species specific and therefore cannot be studied in animal models. As such, a protocol to differentiate microglia (iPSdM) from induced pluripotent stem (iPS) cells was optimized in the scope of this thesis. However, the cell numbers obtained were limited and hindered the extent of biochemical and functional analysis that could be performed. Therefore, THP1 human monocyte-derived macrophage cell line was used as a surrogate human model system to study the role of SIGLEC3 signaling. In this regard, the influence of an immunogenic sialic acid - Neu5Gc in comparison to sialic acid - Neu5Ac, serving as a ligand to SIGLEC3, on macrophage functions was analyzed. Furthermore, in order to mimic the environment of an AD brain on a molecular level, macrophages were also chronically treated with nanomolar concentrations of Aβ. The overall hypothesis of this thesis involves the comprehensive idea that chronic inflammation occurs as a result of persistently activated microglia due to improper SIGLEC3 signaling caused by Neu5Gc. The chronically malfunctioning microglia exacerbates neurodegeneration and elicits an inappropriate response to Aβ

deposition. Overall, this thesis aims at determining the underlying molecular mechanisms preceding clinically diagnosed LOAD.

2. Materials and Methods

2.1 Materials

2.1.1 Cell lines

JS-AF12 iPS	induced pluripotent stem cell line, generated and kindly provided by AG Brüstle, University of Bonn, Germany
SdMic 1	Induced pluripotent stem cell (JS-AF 12) derived microglial line, generated based on protocol from the thesis of Dr. Kristin Roy
SdMic 2	Induced pluripotent stem cell (JS-AF 12) derived microglial line, generated based on protocol from the thesis of Dr. Kristin Roy
THP1 wildtype monocytes (WT)	kindly provided by the group of Prof. Hornung, University of Bonn
THP1 SIGLEC3 knockout monocytes (SIG3 KO)	kindly generated and provided by the group of Prof. Hornung, University of Bonn

2.1.2 Chemicals and Reagents

1,4-Diazobicyclo-(2.2.2)octan	Sigma Aldrich Chemie GmbH, Germany
Accutase (STREM Pro cell dissociation reagent)	Gibco, Thermo Fischer scientific, USA
Amyloid-beta, biotinylated	Bachem, Germany

Amyloid-beta, non-biotinylated	Peptide speciality laboratories, Germany
Apo-transferrin, Human	Sigma Aldrich Chemie GmbH, Germany
Apo-transferrin, Bovine	Sigma Aldrich Chemie GmbH, Germany
Aqua Poly/Mount	Polysciences Inc, USA
β-Mercaptoethanol	Gibco, Thermo Fischer scientific, USA
B27 supplement (50x)	Gibco, Thermo Fischer scientific, USA
Bovine serum albumin	Sigma Aldrich Chemie GmbH, Germany
Collagenase , type IV	Gibco, Thermo Fischer scientific, USA
Chicken serum	Gibco, Thermo Fischer scientific, USA
ddH_2O	Filtered and autoclaved in-house
D-(+)-Glucose solution (45 %)	Sigma Aldrich Chemie GmbH, Germany
DiI, cell tracker	Life technologies, USA
Dihydroethidium (DHE)	Thermo Fischer scientific, USA

Dimethyl sulfoxide	Carl Roth GmbH & Co KG,, Germany
DMEM/F12 (1:1) with L-glutamine and 15 mM HEPES	Gibco, Thermo Fischer scientific, USA
EDTA	Carl Roth GmbH & Co KG,, Germany
Ethanol	Carl Roth GmbH & Co KG, Germany
Fluoresbrite Polychromatic Red microspheres 1.0 µm	Polysciences Incorporated, Germany
Fibronectin from bovine plasma	Sigma Aldrich Chemie GmbH, Germany
Fibronectin 0.1 % solution	Sigma Aldrich Chemie GmbH, Germany
Fetal calf serum	Gibco, Thermo Fischer scientific, USA
Geltrex	Thermo Fischer scientific, USA
Knockout serum replacement	Gibco, Thermo Fischer scientific, USA
Laminin	Sigma Aldrich Chemie GmbH, Germany
L-Glutamine (200 mM)	Gibco, Thermo Fischer scientific, USA
LPS	Invivogen, USA

Non-essential amino acids (10 mM)	Gibco, Thermo Fischer scientific, USA
N2 supplement (100x)	Gibco, Thermo Fischer scientific, USA
Normal goat serum	Sigma Aldrich Chemie GmbH, Germany
Paraformaldehyde	Merck Millipore, Germany
PBS	Gibco, Thermo Fischer scientific, USA
Penicillin/Streptomycin	Gibco, Thermo Fischer scientific, USA
Phorbol 12-myristate 13-acetate	Sigma Aldrich Chemie GmbH, Germany
Poly-L-Lysine	Sigma Aldrich Chemie GmbH, Germany
Poly-L-Ornithin	Sigma Aldrich Chemie GmbH, Germany
ROCK Inhibitor Y-27632	Merck Millipore, Germany
RPMI medium 1640	Thermo Fischer scientific, USA
Sodium pyruvate (100 mM)	Gibco, Thermo Fischer scientific, USA
TritonX	Sigma Aldrich Chemie GmbH, Germany

Trypsin (0.25 %)	Gibco, Thermo Fischer scientific, USA

2.1.3 Growth factors and Cytokines

Recombinant human fibroblast growth factor 2 (rhFGF2)	R&D Systems GmbH, Wiesbaden, Germany
Recombinant human (rh) IL 34	Biolegend,BIOZOL, Germany
Recombinant human Macrophage colony stimulation factors (rhMCSF)	R&D systems, USA

2.1.4 Buffers and Solutions

4 % Paraformaldehyde	4 g Paraformaldehyde in 100 ml 1x PBS
10x Bovine serum albumin	10 g BSA in 100 ml 1 x PBS
10x TBE	108 g Tris 55 g boric acid 40 ml 0.5 EDTA ad 1 l aqua bidest.
EDTA	46.53 g EDTA 170 ml aqua bidest. adjust pH 8.5 with 5 M NaOH ad 250 ml aqua bidest.
MES SDS running buffer for western blot	Novex, Life Technologies, USA

Poly-L-Lysine (5 µg/ml)	5 µg in 1 ml aqua dest.
Poly-L-Ornithin (0.01 mg/ml)	9.2745 g boric acid ad 1 l aqua bi-destilled 100 mg Poly-L-Ornithin
Restore Plus western blot stripping buffer	Thermo Fischer scientific, USA
Saccharose, 30 %	30 % saccharose 0.1 % sodium azide add 500 ml PBS
Transfer buffer for western blot	Novex, Life Technologies, USA
Tris buffer, 0.2 mM pH 8.5	24.765 g in 150 ml aqua bidest. adjust pH

2.1.5 Kits

RNeasy Mini Kit	Qiagen
SuperScript First-Strand Synthesis Systme	Invitrogen
Blood and tissue kit	Qiagen

2.1.6 Media

B27 differentiation medium	APEL medium (StemCell technologies) 2 % B27 20 ng/ml rhFGF2 5 µg/ml fibronectin

freezing medium	50 % KO-SR
	40 % medium
	10 % DMSO
iPS-differentiation medium	DMEM/F12 (1:1) with L-glutamine with HEPES (15 mM)
	20 % knockout serum replacement
	0.1 mM NEAA
	0.1 mM L-glutamine
N2 differentiation medium	APEL medium (StemCell technologies)
	1 % N2 supplement
	20 ng/ml rhFGF2
	10 ng/ml laminin
N2 medium	DMEM/F12 (1:1) with L-glutamine with HEPES (15 mM)
	1 % N2 supplement
	0.5 mM L-glutamine
	5.3 µg/ml D-glucose
	100 µg/ml penicillin/streptomycin
TESR-E8 medium	Stem cell technologies
THP1 medium for monocyte culture	RPMI medium1640 (500 ml)
	1 % chicken serum
	1 % sodium pyruvate
	1 % L-glutamine
	1 % penicillin/streptomycin

	1 % N2 supplement
THP1 experimentation medium	RPMI medium1640 (500 ml)
	1 % sodium pyruvate
	1 % L-glutamine
	1 % penicillin/streptomycin
	1 % N2 supplement

2.1.7 Consumable supplies

6-well Tissue Culture Plate	Cellstar, Greiner Bio One, Germany
96-well optical bottom plates	Thermo Fischer scientific, USA
Bacterial dishes (100 mm)	Corning incorporated, USA
Cell Scraper	Sigma Aldrich Chemie GmbH, Germany
Cryovials (2 ml)	Sarstedt Ag & CoKG, Germany
Falcon tubes (15 ml)	Cellstar, Greiner Bio One, Frickenhausen, Germany
Falcon tubes (50 ml)	Sarstedt Ag & CoKG, Germany
Filtropur (0.25 µm, 0.4 µm)	Sarstedt Ag & CoKG, Germany
Graduate pipette Tipps (10 µl, 100 µl, 1000 µl)	Starlab GmbH, Ahrensburg, Germany
Lab-Tek Chamber Slide w/ Cover Permanox Slide Sterile 4	Thermo Fischer scientific, USA

Well	
Microscope cover glasses	P. Marienfeld GmbH, Germany
Needles	Sterican, Braun Meisungen AG, Germany
Nitrile gloves	Meditrade, Germany
Pasteur pipettes	Brand GmbH & Co KG, , Germany
Pipettes (5 ml, 10 ml, 25 ml)	Corning incorporated, USA
Safe-seal micro tubes (0.5 ml, 1.5 ml, 2 ml)	Sarstedt Ag & Co KG, Germany
Syringes (5 ml, 10 ml)	Omnifix, Braun Meisungen AG, Germany
Tissue Culture Dishes (35 mm, 60 mm, 100 mm)	Sarstedt Inc., USA
Tissue Culture Flask (75 cm^3, 25 cm^3)	Sarstedt Inc., USA
Vacuum driven disposable bottle top filter	Merck Millipore, Germany

2.1.8 Technical equipment

- 20°C freezer	Liebherr, Switzerland
+ 4°C fridge	Liebherr, Switzerland

BD FacsCalibur	BD Biosciences, USA
BD FacsCanto II	BD Biosciences, USA
Cell MateII (pipette boy)	Thermo Fisher Scientific Inc., USA
Eppendorf Mastercycler epgradient S	Eppendorf
Hera cell 150 (incubator)	Heraeus Holding GmbH, Germany
Hera freeze (- 80°C freezer)	Heraeus Holding GmbH, Germany
Hera safe (laminar-air flow workbench)	Kendro Laboratory Products GmbH, Germany
Mefaguge1.0R (centrifuge)	Heraeus Holding GmbH, Germany
Microscopes HBO 50/AC Axiovert200M ImagerZ1	Carl Zeiss AG, Germany
Micropipettes (10µl, 100µl, 1000µl)	Eppendorf AG, Germany
Systec D-150 (autoclave)	Systec GmbH, Germany

Thermomixer compact	Eppendorf AG, Germany
Water bath WB/OB7-45	Memmert GmbH & CoKG, Germany

2.1.9 Software

BD CellQuest Pro	BD Biosciences, USA
BD FACS Diva	BD Biosciences, USA
FlowJo	FlowJo LLC, USA
Fluoview ver.3.1	Olympus corporation
ImageJ	NIH, USA
ImageLab	Bio-Rad, Germany
Olympus FluoView1.4	Olympus, Germany
SPSS	SPSS Inc., USA
Wallac Envision manager	PerkinElmer, USA

2.2 Methods

2.2.1 Culture of induced pluripotent stem cells

Induced pluripotent stem (iPS) cells were cultured on a layer of geltrex matrix in TESR-E8 medium. The iPS cells grow in colonies and when the colonies covered about 70% of the surface, they were passaged using accutase. For passaging, colonies were treated with accutase for 3 minutes. The detached single cells were collected in a falcon tube and centrifuged at 1000 rpm, for 3 minutes. The cell pellet was resuspended in fresh TESR-E8 medium and plated onto a new matrix-coated culture plate in the presence of 10 µM ROCK inhibitor for the first 24 hours after passaging. After 24 hours, medium containing ROCK inhibitor was replaced with fresh pre-warmed TESR-E8 medium.

2.2.2 Generation of induced pluripotent stem cell derived microglial cell lines (iPSdM)

Differentiation was initiated by detaching intact colonies using 1 mg/ml collagenase. The colonies were centrifuged at 1000 rpm, for 3 minutes and the supernatant was discarded. The cell pellet was very gently resuspended, to maintain the colonies intact, in iPS-differentiation medium and placed in non-adherent bacterial culture dishes to support 3-D formation of embryoid bodies (EBs). The EBs were maintained in suspension culture for eight days. On the final day of suspension culture, a few EBs were analyzed for the expression of KDR (1:5, anti-human KDR-FITC) and CD235a (1:50, anti-human CD235a-APC) positive cells, by flow cytometry. The remaining EBs were then plated onto PLO/Fn coated culture dishes in B27 differentiation medium (section 2.1.6) and maintained for 14 days, with media changes as necessary. For the first two days in B27 differentiation media, the differentiating cells were stimulated with 50 ng/ml IL-34. The culture media was then switched to N2 differentiation (section 2.1.6), for a further 10 days. For the first two days in N2 differentiation media, the differentiating cells were stimulated with 50 ng/ml IL-34. Finally, the cells were cultured in N2 medium without supplementation. The differentiation plates were supplied with fresh N2 medium as necessary and maintained in culture until the appearance of microglia was observed. Microglia were morphologically identified as round-shiny cells with a size of 30 - 40 µm. At the appearance of a few round-shiny cells, the differentiation plate was stimulated for 48 hours with IL-34 (100 ng/ml) to support the expansion of the cells of interest. Once several thousand cells appear, the round-shiny cells can be manually isolated with the help of a micropipette and bright-field microscope under a sterile, horizontal hood.

All analyses were carried out on PLL-coated 96-well optical-bottom plates and using confocal microscopy. The morphologically identifiable round-shiny microglial cells were manually isolated from the differentiation plate using a micropipette. The isolated cells were distributed in a 96-well plate and stimulated with IL-34 (100 ng/ml) for the first 24 hours after isolation

2.2.3 Proliferation assay for iPSdM

Proliferative capacity of cells was analyzed by measuring the incorporation of Ki67. The cells were fixed for 10 minutes by 4 % PFA followed by washing and blocking in 10 % BSA supplemented with 0.5 % NGS and 0.1 % Triton-X-100, for 60 minutes at room temperature. After blocking, the cells were co-stained overnight with primary

antibodies against Ki67 and IBA-1, at 4 °C (table 1). Cells were then stained with corresponding secondary antibodies (table 1) for 2 hours at room temperature, protected from light. Finally, the nuclei of the cells were stained with 1:10,000 DAPI for 30 seconds. After washing three times in 1x PBS, cells were stored in 1x PBS and imaged immediately by confocal microscopy. Analyses were performed using ImageJ software.

2.2.4 Immunocytochemical analysis for microglial markers

The isolated microglial cells were placed a 96-well optical bottomed plate and fixed with 4 % PFA for 10 minutes. Following fixation, cells were blocked for 60 minutes at room temperature with 10 % BSA supplemented with 5 % NGS and 0.1 % Triton-X-100. The primary antibodies were added overnight at 4 °C (table 1). Respective secondary antibodies were stained for 2 hours at room temperature, protected from light (table 1). Cells were then kept in 1x PBS and imaged immediately by confocal microscopy. Analyses were performed using ImageJ software.

Table 1: Antibodies for immunocytochemical analysis of iPS-derived microglia

Primary antibody (concentration)	Secondary antibody (concentration)
CD11b (5 µg/ml) **BD biosciences, 553307**	PE anti-rat (5 µg/ml)
TREM2 (5 µg/ml) **R&D systems, mab1828**	PE anti-mouse (5 µg/ml)
Ki67 (1:100) **Millipore, AB9260**	PE anti-rabbit (5 µg/ml)
IBA-1 (1:500) **Wako, 019-19741**	PE anti-rabbit (5 µg/ml)

2.2.5 Culture of THP1 monocytes and macrophages

Wildtype (WT) as well as SIGLEC3 Knockout (SIG3 KO) THP1 monocytes were generously contributed by Prof. Hornung (University of Bonn). SIG3 KO cells were obtained by crispr-cas9 technology, causing a four base pair deletion in Exon 3 (base pair 566 to base pair 569). The deletion disrupts translation of the modified gene into

a functional protein. The SIG3 KO cells are a 100 % devoid of functional protein SIGLEC3.

Monocytes were obtained in RPMI medium supplemented with 10 % FCS, 2 mM L-glutamine, 1 mM sodium pyruvate and 100 µg/ml penicillin/streptomycin. However, further culturing was performed in modified medium adapted to contain only acetylated sialic acids (human-like). For this purpose, culturing was carried out in RPMI medium supplemented with 1 % Chicken Serum, 0.2 mM L-glutamine, 1 mM sodium pyruvate, 100 µg/ml penicillin/streptomycin and 1 % N2 supplement. Experimentation was performed on monocyte-derived macrophages. THP1 macrophages were obtained from monocytes by plating a defined number of cells in culture plates with 10 ng/ml PMA, for 48 hours. After 48 hours, PMA is washed out of the culture by washing cells three times with sterile PBS. Washed cells were then cultured in respective sialic-acid containing medium, as described below.

2.2.6 Sialic acid feeding and chronic amyloid β exposure - experimental setup

For experimentation, monocyte-derived macrophages were cultured in THP1 experimentation containing 0.2 mM L-glutamine, 1 mM sodium pyruvate, 1 % N2 supplement and 100 µg/ml penicillin/streptomycin. As controls, cells were cultured in THP1 experimentation medium without sialic acid supplementation (SDm). Samples include culturing cells in THP1 experimentation medium supplemented with either 6 µM Neu5Ac (ACm) or 6 µM Neu5Gc (GCm). Both Neu5Ac and Neu5Gc were delivered to the cells in the form of protein-bound sialic acid. Appropriate concentration of apo-transferrin bound Neu5Ac and apo-transferrin bound Neu5Gc were supplemented in the cell culture to obtain a final concentration of 6 µM Neu5Ac or 6 µM Neu5Gc, respectively. Fresh medium was exchanged every alternative day for a total of 6 days.

Additionally, a day after having started the sialic acid supplementation, cells were either left untreated or treated with 0.25 µM non-biotinylated amyloid β (nbAβ). Chronic exposure was achieved by adding Aβ every day, until day 6. On day 6, respective experiment was performed.

Preparation of Aβ, for chronic treatment was performed as follows. The non-biotinylated Aβ was commercially obtained from Peptide specialty laboratories in the form of lyophilized powder. Lyophilized Aβ was resuspended in sterile water to a

concentration of 1100 µM and stored at -20°C. Before addition to the cell culture, Aβ was incubated at 37°C for 7 days with vortexing every day for 2 - 3 minutes. Pre-incubated Aβ was then diluted to 100 µM in sterile water and stored as aliquots at -20°C. Aliquots were thawn and vortexed prior to use in cell culture.

Table 2: Experimental Setup for sialic acid feeding and chronic Aβ treatment

day x - 2	differentiate monocytes into macrophages by 10 ng/ml PMA treatment for 48 hours
day 0	wash out PMA and culture cells in respective sialic-acid supplemented medium (SDm, ACm or GCm)
day 1	untreated or 0.25 µM nbAβ
day 2	media change with respective sialic acid supplementation, untreated or 0.25 µM nbAβ
day 3	media change with respective sialic acid supplementation, untreated or 0.25 µM nbAβ
day 4	media change with respective sialic acid supplementation, untreated or 0.25 µM nbAβ
day 5	media change with respective sialic acid supplementation, untreated or 0.25 µM nbAβ
day 6	Experimentation

2.2.7 HPLC

The incorporation of Neu5Ac and Neu5Gc from the respective supplemented medium was analyzed by xCGE-LIF (multiplexed capillary gel electrophoresis with laser-induced fluorescence detection) and Flow cytometry.

For xCGE-LIF analyses, 5 x 10^5 cells were seeded per well of a 6-well plate. One well was seeded per condition, as described in table 2. On day 6, cells were scraped and pelleted by centrifugation at 1300 rpm, for 3 minutes. Supernatant was discarded and the pellets were resuspended in 200 µl RIPA buffer containing 2 µl HALT protease-phosphatase inhibitor cocktail. The cell suspensions were stored at -80°C

till analysis. Three repeats of the above described procedure were performed. xCGE-LIF analysis was performed in cooperation with collaborators at the Max Planck Institute for Dynamics of Complex Technical Systems, Magdeburg. In short, the precipitated proteins were concentrated by affinity-solid phase extraction and separated on a 2-D gel electrophoresis system. The bands were then cut out and the N-glycan structures were extracted from the gel, in water by PNGase F enzyme activity. The extracted N-glycans were then fluorescently labeled with APTS (9-aminopyrene-1,4,6 trisulfonic acid) and run on a UPLC system to detect the Neu5Ac and Neu5Gc present on the N-glycan structures.

2.2.8 RNA sequencing analysis

RNA sequencing analysis of samples from cells cultured in SDm, ACm and GCm were performed by the group of Prof. Joachim Schultze (University of Bonn, Limes). After the six day culture (table 2), each sample was centrifuged to obtain cell pellets. Cell pellets were then resuspended in 1 ml Qiazol each and stored at -80°C before RNA extraction, measurement and analysis. RNA sequencing was performed for the three out of four individual samples with the highest quality, as measured using TapeStation. In short, template libraries were made from double stranded cDNA molecules obtained from total RNA. Further downstream processing and analysis were performed as described by the following publications; (Fujita et al. 2011)(Trapnell et al. 2009)(Trapnell et al. 2010)(Langmead et al. 2009) and (Trapnell et al. 2012).

2.2.9 Flow cytometry analyses

Cell numbers and antibodies used are specific to each experiment as described in table 3.

For flow cytometry analysis of **Neu5Gc incorporation**, chicken polyclonal antibody directed against Neu5Gc was used. 1 x 10^6 cells were seeded per well of a 6-well plate, one 6-well plate was seeded per cell line (WT and SIG3 KO). On experimentation day, cells were scraped and pelleted by centrifugation at 1300 rpm, for 3 minutes. The pellets were resuspended in diluent buffer with or without 1:500 Neu5Gc antibody, as provided by the manufacturer. Primary antibody staining was performed at room temperature for 1.5 hours. Cells were washed by centrifugation. A secondary antibody, biotin anti-chicken (5 µg/ml) was added for 45 minutes, on ice.

Cells were washed by centrifugation. A fluorescently labeled tertiary antibody, PE-streptavidin (5µg/ml) was added for 30 minutes on ice, protected from light. Relative fluorescence intensity was measured by Flow cytometry and analyses were performed using FlowJo software.

For calculating ***cis*-bound SIGLEC3** as well as **surface marker analysis**, 1 x 10^6 cells were seeded per well of a 6-well plate. One 6-well plate was seeded per cell line (WT and SIG3 KO). On experiment day, macrophages were washed once with sterile 1x PBS to remove debris. Cells were then detached from culture plates using cell scrapers and pelleted by centrifugation at 1300 rpm, for 3 minutes. Cell pellets were resuspended in 1x PBS and respective primary antibody was added (table 3). Cells were stained with primary antibody for 1 hour, on ice. Samples were then washed by centrifugation with 1x PBS. After washing, samples were resuspended in 1x PBS and respective secondary antibody for 30 minutes, on ice and protected from light. Finally, the cells were washed by centrifugation and resuspended in 200 µl 1x PBS, measured by FACS calibur and analyzed using FlowJo software.

Apoptosis assay was performed to find the apoptotic rate of cells under the different culture conditions. Apoptosis assay was performed on monocytes and not macrophages. Apoptosis was measured by staining with Annexin V antibody. 5 x 10^5 monocytes were seeded in a 25 cm^3 culture flask. On experiment day, cells were pelleted by centrifugation at 1300 rpm, for 3 minutes. Pellets were resuspended in 100 µl of freshly made 1x binding buffer (diluted from the stock of 10 x binding buffer: 0.1 M HEPES, pH7.4, 1.4 M NaCl, 25 mM $CaCl_2$). Cells were once again pelleted by centrifugation. Supernatant was discarded and pellet was resuspended in 100 µl 1x binding buffer containing 2.5 µl Annexin V antibody, per sample. Incubation with primary antibody was carried out for 15 minutes at room temperature. Cells were then washed in 1x binding buffer, by centrifugation as described above. Cells were resuspended in 100 µl 1x binding buffer containing 1:500 PE-streptavidin, per sample for 30 minutes on ice, protected from light. Cells were washed in 1x binding buffer, by centrifugation as described above and fluorescence intensity was measured by Flow cytometry and data was analyzed by FlowJo software.

Table 3: Antibody list for Flow cytometry analysis

Experiment	Primary antibody (concentration)	Secondary antibody

(corresponding result section)		(concentration)
Neu5Gc incorporation	polyclonal chicken anti-Neu5Gc (1:500); Biotin anti-chicken (5 µg/ml)	PE streptavidin
***cis*-bound SIGLEC3 detection**	mouse anti-SIGLEC3, clone WM53 (5 µg/ml) mouse anti-SIGLEC3, clone HIM3-4 (5 µg/ml)	PE anti-mouse
Apoptosis assay	biotinylated anti-Annexin V (1:50)	PE streptavidin

2.2.10 Western Blot

1 x 10^6 cells were seeded per well of a 6-well plate, per cell line (WT and SIG3 KO). Cells were treated as described in table 2. On the day of experimentation, cells were detached using cell scraper and pelleted by centrifugation. Each pellet was resuspended in 100 µl RIPA buffer containing 2 µl HALT proteases and phosphatases cocktail. Samples were incubated on ice for 1 hour and cellular debris was removed by centrifugation at 12000 rpm, for 15 minutes. Supernatant containing whole cell lysate was used to immunoprecipitate specific proteins for further analysis as described in table 4. Proteins were immunoprecipitated using either protein A or protein G dynabeads (ThermoFischer), per manufacturer's protocol. After immunoprecipitation of the protein-of-interest, LDS loading buffer was added to the samples and heated for 10 minutes at 75 °C. Samples were directly loaded from the heating block, onto 10 % BIS-TRIS SDS PAGE and run in standard MES running buffer at 130 volts for 1.5 hours. Proteins were then transferred from the gel onto activated nitrocellulose blots in transfer buffer (40 ml 20x-NuPAGE transfer buffer diluted in 80 ml methanol and 680 ml ddH_2O) for 1 hour at 380 mA. Blots were then blocked for 1 hour in TBST and stained overnight with first primary antibody diluted in TBST, at 4 °C (table 4). After overnight incubation, blots were washed three times for a total of 15 minutes in TBST. Blots were then incubated with respective secondary antibody (1:10,000) for 1 hour at room temperature followed by washing in TBST as described above (table 4). In some cases, a tertiary antibody was required – as described in table 4 – for which the stained procedure was carried out similar to that of the secondary antibody. After incubation with HRP-coupled antibody, the blots

were visualized using Super Signal Pico kit, per manufacturer's protocol. Bands were detected using BioRad ChemiDoc XRS+ Molecular Imager and analyzed by ImageLab software. Blots were then striped off antibodies by rotating in striping buffer for 30 minutes at room temperature, washed for 15 minutes and blocked for 1 hour, in TBST. Following blocking, blots were stained in second primary antibody, as described in table 4. In general, the second primary antibody was the same as the antibody used for immunoprecipitation. This procedure was performed to normalize the first protein that was stained for, due to the lack of housekeeping protein for normalization. Secondary antibody staining, and if necessary tertiary antibody staining, was performed as described above.

Table 4: Antibody list for Western blot analysis

Experiment (corresponding result section)	**Antibody for immunoprecipitation (concentration)**	**1st and 2nd primary antibody (concentration)**	**secondary and tertiary antibody (concentration)**
SHP1 recruitment to SIGLEC3	mouse anti-SIGLEC 3, clone HIM3-4 (5 µg/ml)	mouse anti-SHP1 (2.5 µg/ml)	**2ry ab:** biotin anti-mouse (1 µg/ml);
		mouse anti-SIGLEC3, clone HIM3-4 (1 µg/ml)	**3ry ab:** HRP streptavidin (1 µg/ml)
phosphoERK detection	Total ERK (1:500)	phosphoERK (1:1000)	HRP anti-rabbit (1 µg/ml)
		TotalERK (1:1000)	

2.2.11 ROS production analysis by DHE staining

Production of reactive oxygen species (ROS) was measured by DHE incorporation and detected using Flow cytometry. WT and SIG3 KO cells were seeded at a density of 70,000 cells per chamber onto 4 chambers of a chamber slide, per cell line. On day of experimentation, all chambers were treated with DHE (1:1000) in KREBS-HEPES buffer for 15 minutes, protected from light. Cells were then immediately washed twice with 1x PBS and fixed using 4 % PFA and mouted with Mowiol-488. Slides were stored at 4 °C and imaged within 24 hours of staining by confocal microscopy. Triplicate images were taken per condition and analyzed using ImageJ

software. Area and integrated density of each image was measured, as well as mean fluorescence intensity of background. Normalized fluorescence intensity per image was calculated as follows:

Area * Mean fluorescence intensity $_{(background)}$ – integrated density

Values obtained were normalized to the WT SDm untreated condition for each experiment. Data was obtained in collaboration with and is described in the Master thesis of Omar Mossad.

2.2.12 Phagocytosis assay

Phagocytic capacity of cells was analyzed by the intake of fluorescently labeled biotinylated Aβ. Macrophages were seeded at a density of 70,000 cells per well on 4-well chamber slides. After culture of macrophages under the respective conditions, cells were treated with biotinylated fibril Aβ for 1.5 hours at 37°C. After incubation, cells were gently washed twice with sterile 1x PBS and fixed for 10 minutes with 4 % PFA. After fixing, cells were washed with 1x PBS and blocked in 10 % BSA containing 5 % NGS and 0.1 % Triton-X-100. Cells were then stained with primary antibody against CD11b (rat anti-human CD11b, 5 µg/ml), overnight at 4 °C. On the next day, cells were washed twice with 1x PBS and incubated in secondary antibody Alexa fluor-488 anti-rat (1:500) and Cy3-streptavidin (1:500) for 90 minutes at room temperature, protected from light. Cells were washed twice with 1x PBS and mounted using Mowiol 488. Slides were stored at 4 °C till imaging. Imaging was performed using Confocal microscopy. Five images were taken per condition and analyzed using ImageJ software. Total number of cells and the number of cells with internalized Aβ were counted. Phagocytic rate was calculated as a ratio of phagocytic cells normalized to the total cell number per image.

2.2.13 Real time PCR

Gene transcription of complement component 3 (*c3*) and complement component 1q (*c1q*), was analyzed by real-time PCR. 5 x 10^5 cells were seeded per well of a 6-well plate. One well was seeded per condition and per cell line as described in table 2. On day of experimentation, cells were detached by scraping and pelleted by centrifugation at 1300 rpm, for 3 minutes. The pellets were then resuspended in 1 ml Qiazol and RNA was isolated by the classical chloroform-phenol technique. Isolated RNA was transcribed into cDNA by Superscript reverse transcriptase III. The

obtained cDNA was measured for impurities by 230/260 and 280/260 values using Nanodrop 1000. 100 ng of cDNA, per sample, was run as triplicates with respective primers (table 5), SYBRgreen and at annealing temperature 60 °C, to obtain Ct values. Obtained values were calculated using the standard ΔΔCt method. All values were normalized to the housekeeping gene *gapdh*. Data was obtained in collaboration with and is described in the Master thesis of Omar Mossad.

Table 5: Antibody list for Western blot analysis

gene	forward sequence	reverse sequence
c1q	GCCCCGCAGTGGCAAGTTCA	ACCTTCTGTGCACGCTCCCG
c3	GAGGTCATAGTGGAGCCTACA	GGTTAGAGACTGCACAGTGTC
gapdh	CTGCACCACCAACTGCTTAG	TTCAGCTCAGGGATGACCTT

2.2.14 Statistics

All experiments were repeated at least 3 times and obtained data was checked for statistically significant differences using SPSS software by ANOVA test with Bonferroni correction. Significance was illustrated as * ($p \leq 0.05$), ** ($p \leq 0.01$), *** ($p \leq 0.001$) and n.s (not significant).

3. Results

3.1 Developing human microglia from iPS cells as an in vitro model to study SIGLEC3

The study of human microglia under healthy as well as pathological conditions requires a stable supply of microglia for functional and biochemical analysis. Limitations in number of primary microglia and abnormal alterations in primary microglial cell lines obtained by viral transduction hinder these analyses. Therefore, a differentiation protocol to obtain microglial cell lines from iPS cells was performed based on the protocol from Beutner and colleagues (Beutner et al. 2010), which describes differentiation of mouse microglial lines from mouse embryonic stem cells. A healthy iPS cell line, JS-AF12 was used to obtain Stem cell-derived microglial (SdMic) lines 1 and 2 (SdMic 1 and SdMic 2), which represent microglia in healthy individuals. The differentiation procedure of SdMic lines was performed as described in the Doctoral thesis of Dr. Kristin Roy (Roy 2012).

The derived SdMic lines proved to be genetically instable. The instability of these lines was confirmed by increased chromosomal numbers in SdMic1 and SdMic2 in comparison to the JA-AF12 iPS cells from which they were generated (figure 7A). While the iPS cell line carried on average 46 chromosomes (46 ± 2.5) as expected for human material, microglial lines SdMic1 and SdMic2 carried 55 ± 2.3 and 53 ± 2.8 chromosomes, respectively. Furthermore, SNP analysis of both microglial lines showed erroneous results as seen in figure 7B, in comparison to the iPS line JS-AF12 from which they were generated.

Therefore, an attempt to develop genetically stable and reproducible microglial cells was made in the scope of this thesis and is described below.

Contrary to the previously described protocol, iPS cells (JS-AF 12) were cultured on a basement membrane matrix; namely Geltrex. All steps of the differentiation protocol are illustrated in figure 7C. The stem cells, cultured in TESR-E8 medium, formed colonies (figure 7C-1). The EBs formed were between 200 and 300 µM in size (figure7C-2) and were a combination of ectodermal, endodermal and mesodermal tissue as described in literature (schematic image, figure 7C-3). On the final day of

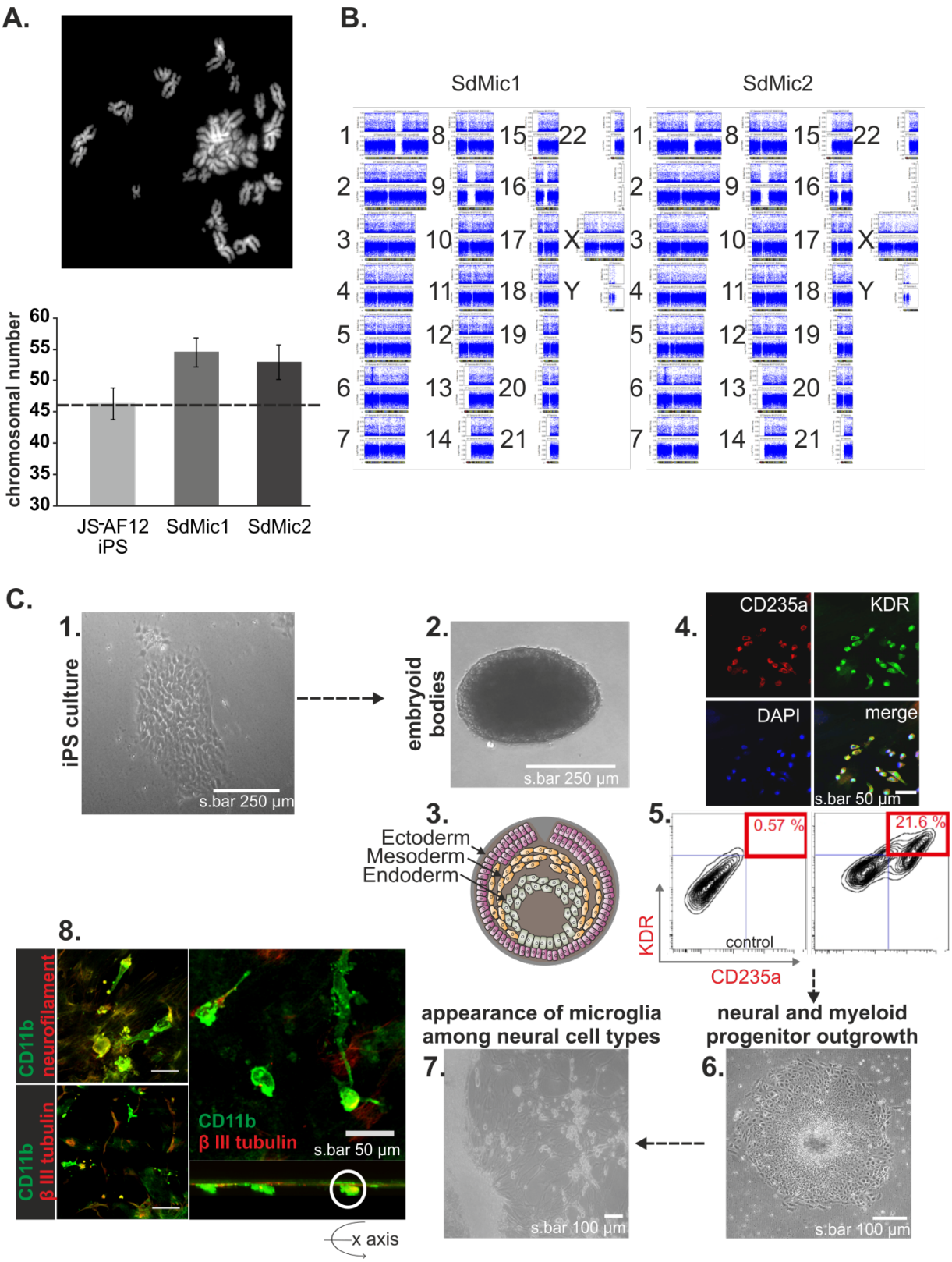

Figure 7: Previously generated SdMic lines 1 and 2 carry an increased number of chromosomes in comparison to the expected 46 chromosomes as seen in human material. While the JS-AF iPS from which SdMic1 and SdMic2 were generated carried 46 ± 2.5 chromosomes on average, SdMic1 and SdMic2 lines carried 55 ± 2.3 and 53 ± 2.8 chromosomes, respectively (A). Additionally, both SdMic lines have disrupted single nucleotide polymorphism (SNP) profile (B).

Modified protocol to obtain proliferative induced pluripotent stem cell derived microglia (iPSdM) (C) includes culturing of stem cells on a matrix-layer (C, 1) and developing embryoid bodies (C, 2), consisting of all three germ layers (representative image C,3) that are double positive for KDR and CD235a, as seen by immunocytochemical staining (C, 4; representative image of at least 3 independent experiments) and flow cytometry analysis (C, 5). On average, 21.6 % ± 0.5 % of EBs were positively co-stained for KDR and CD235a (C, 5). Development of neural and myeloid progenitors out of the EBs was supported (C, 6) and further differentiation into final cell types was initiated (C, 7). The differentiated microglia were positive for marker CD11b and were found among β-III-tubulin and neurofilament positive neural cell types. When rotated on the x-axis, a phagocytic microglia with internalized β-III-tubulin particles can be observed.

suspension culture, the EBs were analyzed for the expression of KDR and C235a positive cells. Immunocytochemical analysis revealed co-localization of KDR and CD235a staining. Flow cytometry analysis revealed that $KDR^{+}CD235a^{+}$ double positive cells made up around 21.6 % ± 0.5 % of the total population, in comparison to isotype control; 0.5 % ± 0.0 % (figure 7C-5). The presence of double positive cells is indicative of primitive hematopoeisis, from which microglial cells arise. The absence of $KDR^{+}CD235a^{-}$ cells indicated the absence of definitive hematopoeisis, from which peripheral macrophages and monocytes arise. EBs were then plated and directed to differentiate into neural and myeloid progenitor cell types (figure7C-6). The culture medium was switched to N2 medium supplemented with laminin and growth factor - rhFGF2. At this stage, the neural precursors were supported to develop into neural cell types and the myeloid precursors were supported to develop into primitive microglial cells (figure 7C-7). In the final stage of differentiation, cells were cultured in N2 medium in the absence of growth factors to support spontaneous differentiation of precursors into final cell types; microglial cells develop among other neural cell types (β III tubulin^{+}; neurofilament^{+}, figure 7C-7). Differentiation of microglia can develop at time points of up to 4 months after the initiation of differentiation. Microglial cells in the differentiation culture plates were morphologically identified as round-shiny cells of about 30 - 40 µm. The CD11b-positive microglial cells develop alongside β III tubulin-positive neural cell types. In fact, preliminary indications of the phagocytic capacity of the microglial cells were observed by the presence of red-labeled β III tubulin elements within the green-labeled microglia - as seen by z-stack analysis using confocal microscopy, when the image is rotated on its x-axis (figure 7C-8). The disadvantageous factor in the differentiation protocol was the limited number of microglial cells that developed per

EB. A rough estimate of a few thousand microglial cells per EB can be assumed. This disadvantage limits the extent of molecular analysis that can be performed. Nevertheless, increased microglial cell numbers possibly might be obtained by up-scaling the EB seeding procedure.

3.2 Characterizing microglial cells obtained from human iPS cells

The generated microglial cells were named as induced pluripotent stem cell derived microglial cells 9 (iPSdM9). The microglial cells iPSdM9 were characterized based on proliferation rate and expression of typical microglial surface markers. Due to the limited cell numbers, the characterizations were performed in 96-well optical bottom plates as described in the materials and methods (sections 2.2.3 and 2.2.4).

3.2.1 Immunocytochemical analysis

Mechanically isolated microglial cells were positively stained for typical microglial markers such as CD11b, ionized calcium-binding adapter molecule-1 (IBA-1) and TREM2 (figure 8). The percentage of positive cells for each marker was calculated of the total number of cells from up to 7 individual images. Of the total cells, 36.84 % were positive for CD11b; 47.67 % were positive for marker IBA-1 and 54.55 % were positively stained for TREM2 (figure 8). Total number of cells per image was calculated from the number of nuclei identified by DAPI staining.

3.2.2 Proliferative capacity

The proliferative capacity of the cells was observed by Ki67 incorporation as seen by immunocytochemical staining and analyzed by confocal microscopy. Preliminary data shows that CD11b positive cells can incorporate Ki67, which indicates their ability to proliferate. However, detailed analysis of their proliferation rates need to be analyzed.

In conclusion, the iPSdM9 cells could serve as a well represented alternative to primary human microglia, although cell number is very limited. The cells express typical microglial surface markers and preliminary data indicates that these cells are capable of phagocytosis and proliferation. However, further characterization of the cells is required. While the proliferative capacity of the cells would allow for *in vitro*

expansion, the number of cells obtained was insufficient for analyses of SIGLEC3 by molecular techniques as required by this project.

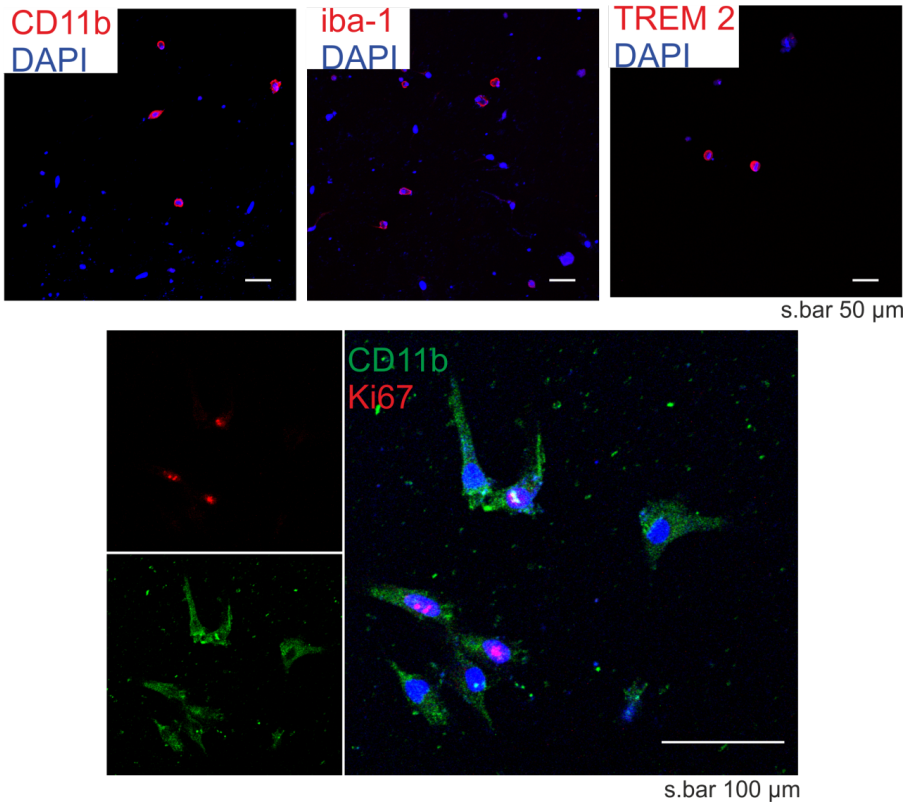

Figure 8: iPSdM9 express microglial markers and are proliferative. The iPS derived microglia (iPSdM9) positively stain for typical microglial markers CD11b, IBA-1 and TREM2 (A). In addition, iPSdM9 incorporate Ki67 in their nuclei, which is an indication of the proliferative capacity of the cells (B). Cells were identified in all images by nuclei staining by DAPI.

3.3 THP1 macrophages as human in vitro model to study SIGLEC3

As discussed above, appropriate representative cell lines for primary human microglia are unavailable in sufficient numbers for functional and biochemical analysis. Due to this restriction, the currently most widely used human macrophage cell line was chosen as a human *in vitro* model to study SIGLEC3 and its signaling. Although microglia and macrophages develop from different phases of hematopoiesis, the final cell types show substantial overlap in terms of surface maker expression profile and functional capabilities. For all intents and purposes, the THP1 monocyte-derived macrophage cell line possesses very similar functional

characteristics typical for phagocytes including the expression of functional human SIGLEC3. As previously stated, the protein of interest in this project is SIGLEC3. Therefore, particular focus was placed on deciphering whether the influence of incorporated sialic acids was mediated through SIGLEC3. For this purpose, all following experiments were performed on both wildtype (WT) THP1 cells as well as on SIGLEC3 knockout (SIG3 KO) THP1 cells.

Collaborators at the research group of Prof. Dr. Hornung used crispr-cas9 to cause a 4 base pair deletion from position 566 to 569 of the SIGLEC3 gene sequence (figure 9A). The deleted region lies in exon 3 of the SIGLEC3 coding sequence and results in the absence of functional SIGLEC3 on the cell surface (figure 9B). Flow cytometry analysis with antibody against SIGLEC3 (clone WM53) shows a reduction of SIGLEC3 surface expression from 45.4 % to 0 % (subtracted from control antibody staining), as seen in example figure 9B (add figure).

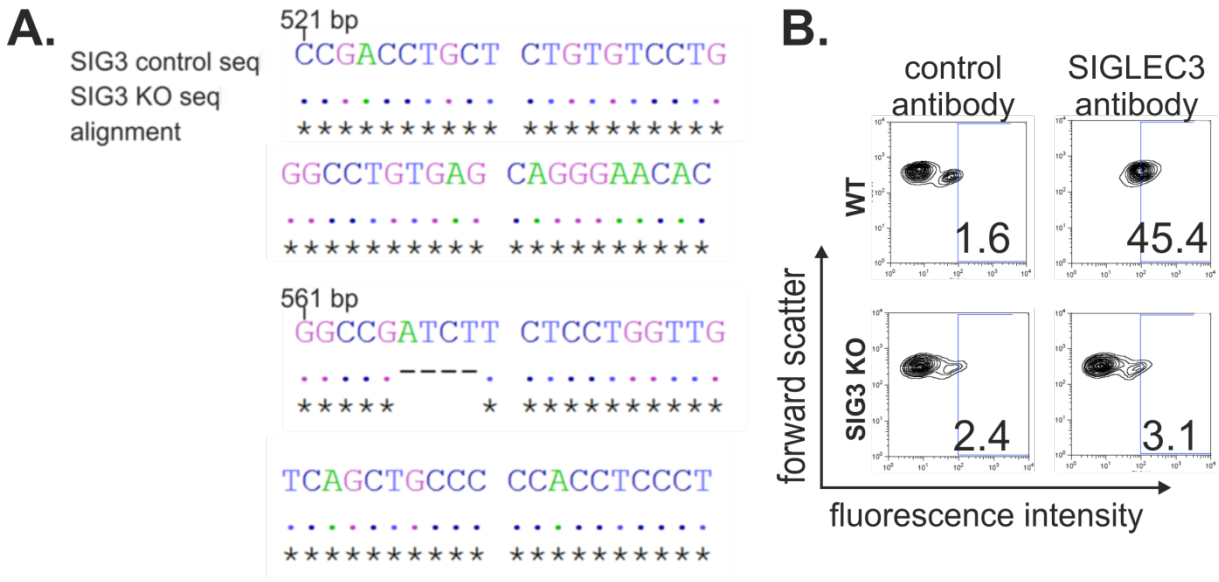

Figure 9: SIG3 KO cells carry a 4 base pair deletion rendering SIGLEC3 protein non functional. Collaborators from the group of Prof. Dr. Hornung (university of Bonn) successfully introduced a 4 base pair deletion in exon 3 of the SIGLEC3 gene using crispr-cas9 technology into THP1 cells. The deletion ranges from base pair 566 to base pair 569, marked as hyphens in comparison to SIGLEC3 control sequence obtained from NCBI (ref seq. NM_001772.3) and aligned using GENtle software (A). Consequently, staining with SIGLEC3 antibody in SIG3 KO THP1 cells confirmed the absence of the protein in comparison to WT THP1 cells. Control antibodies determine unspecific staining (B).3.4 Effects of human sialic acid (Neu5Ac) versus non-human sialic acid (Neu5Gc) incorporation into cell surface glycocaylx

3.4 Influence of sialic acids on functions of THP1 macrophages

3.4.1 Incorporation of Neu5Ac and Neu5Gc into the cellular glycocalyx of THP1 macrophages

As described under the methods section, experiments were performed on THP1 cells cultured in either Neu5Ac containing-medium (ACm) or Neu5Gc-containing medium (GCm). As control, cells were cultured in medium lacking additional sialic acids - named as sialic acid depleted medium (SDm). THP1 macrophage cells were cultured in GCm to mimic the cellular and molecular environment in which non-human sialic acids, metabolically incorporated through consumption of red meat and milk products, could accumulate and consequently affect SIGLEC3 function.

First, incorporation of Neu5Gc into the cell surface glycocalyx of THP1 macrophages was analysed. The macrophages cultured in either ACm or GCm incorporated either Neu5Ac alone or a combination of Neu5Ac and Neu5Gc, respectively. These results were obtained by flow cytometry analysis and xCGE-LIF technique, as described below.

Flow cytometry analysis of Neu5Gc. THP1 WT as well as SIG3 KO cells cultured in GCm were positively stained for Neu5Gc (16.4 % ± 0.85 %). On the other hand, when both cell lines were cultured exclusively in ACm, no Neu5Gc staining was visible (2.1 %) in comparison to secondary antibody controls (1.5 %, representative image in figure 10A). Chronic exposure to fibrillary Alzheimer disease associated amyloid- β (Aβ) to cells significantly increased the appearance of Neu5Gc on the cell surface for both WT and SIG3 KO cells to 39.7 % ± 1.5 % and 24.9 % ± 1.3 % respectively, in comparison to untreated WT and SIG3 KO cells at 16.0 % ± 0.9 % and 12.7 % ± 1.7 %, respectively (figure 10B).

The comparable expression of Neu5Gc in both WT and SIG3 KO in untreated cells indicates that SIGLEC3 does not influence the uptake and incorporation of this glycan. However, Neu5Gc staining significantly increased when both cell types was chronically exposed to low concentrations of Aβ. While SIG3 KO cells chronically treated with Aβ tended to incorporate lower levels of Neu5Gc, the difference was insignificant compared to WT cells chronically treated with Aβ.

XCGE-LIF analysis. While flow cytometry data detects total Neu5Gc on the cell surface, a second technique – xCGE-LIF was performed to identify the presence of Neu5Gc incorporated *exclusively* in total proteins. Collaborators from the group of Dr. Erdmann Rapp (MPI-DCTS, Magdeburg) confirmed the above mentioned flow cytometry results using the advanced xCGE-LIF technique (representative image, figure 10C). Total proteins extracted from cells cultured in either ACm or GCm were analyzed for the presence of Neu5Ac or Neu5Gc sugars. The former expressed 100 % ± 0.0 % Neu5Ac while the latter sample carried 1.2 % ± 0.0 % of Neu5Gc and 98.8 % ± 0.0 % of Neu5Ac sugars, (figure 10D).

Therefore, it can be concluded that Neu5Gc is effectively taken up by the macrophages and expressed on the cell surface. Neu5Gc found on the cell-surface glycocalyx can be available as a ligand for sialic-acid binding receptors. The discrepancies in the percentages of Neu5Gc expression between flow cytometry data and xCGE-LIF data can be explained by the fact that exclusively protein-bound Neu5Gc is measured in the latter case. Therefore it is vital to repeat the xCGE-LIF analysis to detect Neu5Gc on total lipid content to obtain overall quantities. Nevertheless, despite modest percentages of Neu5Gc incorporation, it is sufficient to cause disruption in several cellular processes as seen by RNA sequencing analysis described in section 3.4.2.

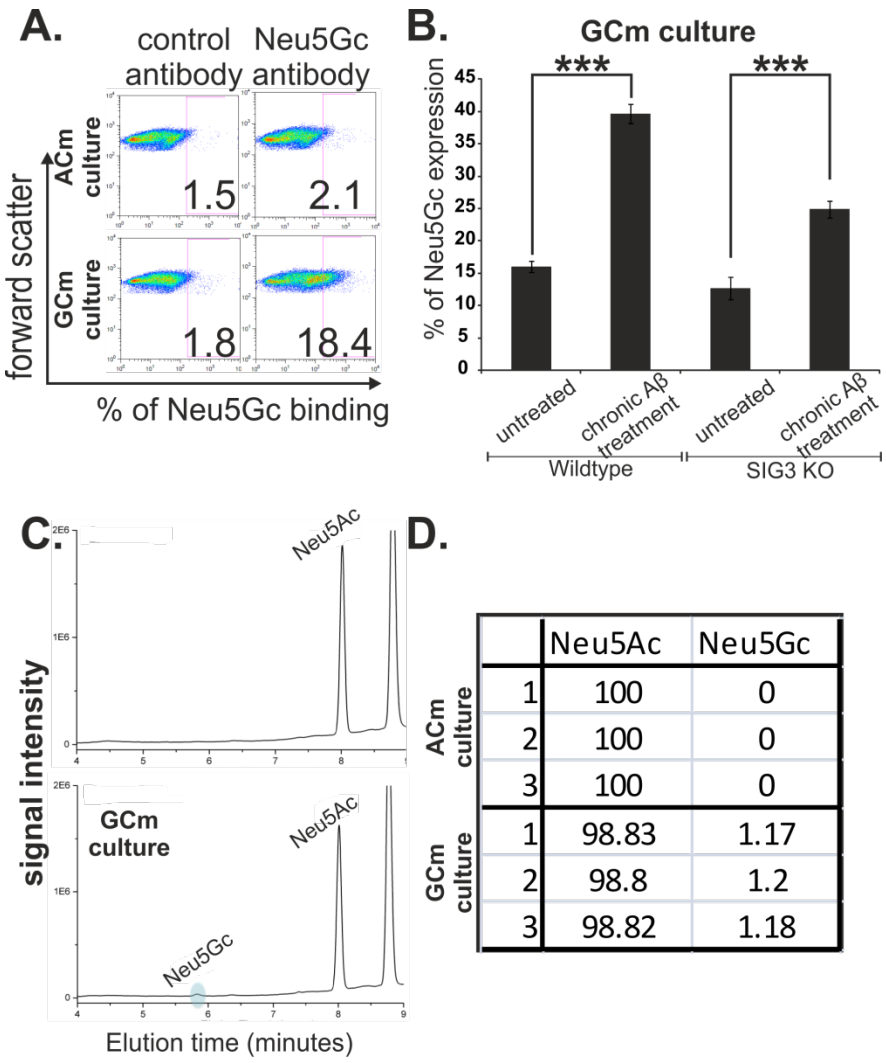

		Neu5Ac	Neu5Gc
ACm culture	1	100	0
	2	100	0
	3	100	0
GCm culture	1	98.83	1.17
	2	98.8	1.2
	3	98.82	1.18

Figure 10: Neu5Gc can incorporate in cells cultured in GCm. Flow cytometry analysis for Neu5Gc detection was performed using a specific chicken polyclonal antibody. Neu5Gc was positively stained in GCm cells but not ACm cells. Control antibody determines unspecific staining (A; representative image of at least 3 independent experiments). Both WT and SIG3 KO effectively incorporated Neu5GC at 16.0 % ± 0.9 % and 12.7 % ± 1.7 %, respectively. In both cell lines, chronic treatment with Aβ significantly increased Neu5Gc incorporation to 39.7 % ± 1.5 % and 24.9 % ± 1.3 %, respectively (B). Detailed analysis exclusively on glycoproteins using xCGE-LIF technique confirmed Neu5Gc incorporation in GCm and not ACm cultured cells (C; representative image of at least 3 independent experiments). Measurement by xCGE-LIF of cultured cells from three independent experiments was quantified (D). n=3.

3.4.2 Incorporated Neu5Gc causes broad cellular dysregulation

In collaboration with the group of Prof. Dr. Schultze (LIMES, Bonn) used RNA sequencing for an in-depth analysis of the influence of Neu5Ac and Neu5Gc incorporation. RNA sequencing analyses revealed that SDm cultured control cells clustered closely with ACm cultured cells, while GCm cultured cells showed several

differentially expressed genes (figure 11A). Of the differentially expressed genes, a total of 768 genes were up-regulated and a total of 707 genes were down-regulated in GCm cells compared to a combination of ACm and SDm cells. On the other hand, only 60 and 39 genes were up- and down-regulated in ACm compared to SDm, respectively. The genes listed were of fold change 1.5 and higher. Particularly, proto-oncogene candidate BLC3 and regulator of cell growth and division EP300 were up-regulated in GCm cells. Furthermore, GO enrichment analysis highlighted several pathways, such as cellular signaling, regulation of immune responses, immune cell development and responses to stimuli, which were altered in GCm cells compared to ACm cells (figure 11B).

Therefore, incorporation of immunogenic Neu5Gc disrupts cellular processes on a wide scale leading to a dysfunctional cellular signaling and immune response from the cells.

3.4.3 Incorporated sialic acids can bind SIGLEC3 and chronic treatment with Aβ increases binding to SIGLEC3

To elucidate the binding capacity of SIGLEC3 to both Neu5Ac and Neu5Gc sugars, SIGLEC3 Fc-fusion protein binding was measured by flow cytometry. Wildtype THP1

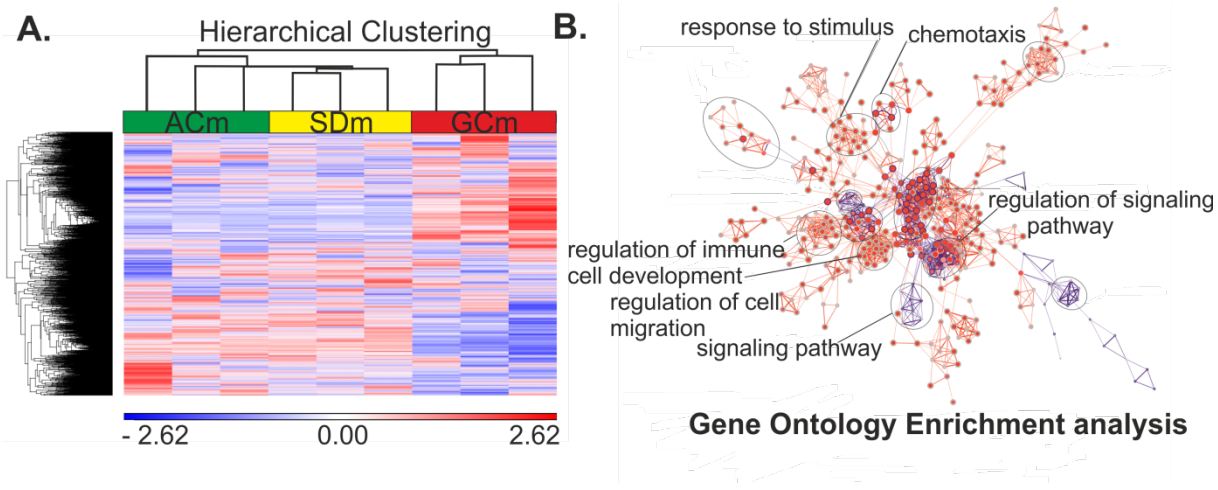

Figure 11: Neu5Gc incorporation causes wide-spread cellular dysregulation.
Heat map analysis of differentially expressed genes shows that ACm clusters to control - SDm, while GCm cultured cells cluster away (A). Gene ontology enrichment analysis highlights several pathways, including cellular signaling, regulation of immune responses, immune cell development and responses to stimuli, which are dysregulated in GCm cultured cells compared to ACm cultured cells (B). n=3.

monocyte-derived macrophages cultured under ACm or GCm bound SIGLEC3 Fc-fusion protein to the same extent (56.8 % ± 2.7 % and 62.5 % ± 4.4 %, respectively). The percentage of binding was significantly increased in cells that were chronically exposed to Aβ, irrespective of the type of sialic acid incorporated (75.0 % ± 0.4 % and 72.1 % ± 2.4 %, respectively) (figure 12A). Therefore, the data obtained confirms that both incorporated sialic acids, Neu5Ac as well as Neu5Gc, can bind to SIGLEC3 Fc-fusion protein. Additionally, the increase in SIGLEC3 Fc-fusion protein binding under chronic exposure to Aβ correlates well with the increased expression of its ligand, namely, sialic acids as seen above (section 3.3.1; figure 10B).

SIGLEC3 expression: ligand-bound protein versus total protein. Like other members of the SIGLEC family, SIGLEC3 can constitutively interact with cis-bound sialic acids. From literature, it is known that a small percentage of SIGLEC3 receptors are bound in cis, to self-ligands, to maintain a baseline homeostatic inhibitory signal. Using two SIGLEC3 antibody clones with different binding epitopes, the percentage of cis-bound SIGLEC3 was determined. Clone WM53 binds to a unique epitope on the protein, which is independent of ligand binding, therefore total protein expression, can be elucidated. A second available clone; HIM3-4 binds an epitope close to the ligand-binding epitope of the protein.

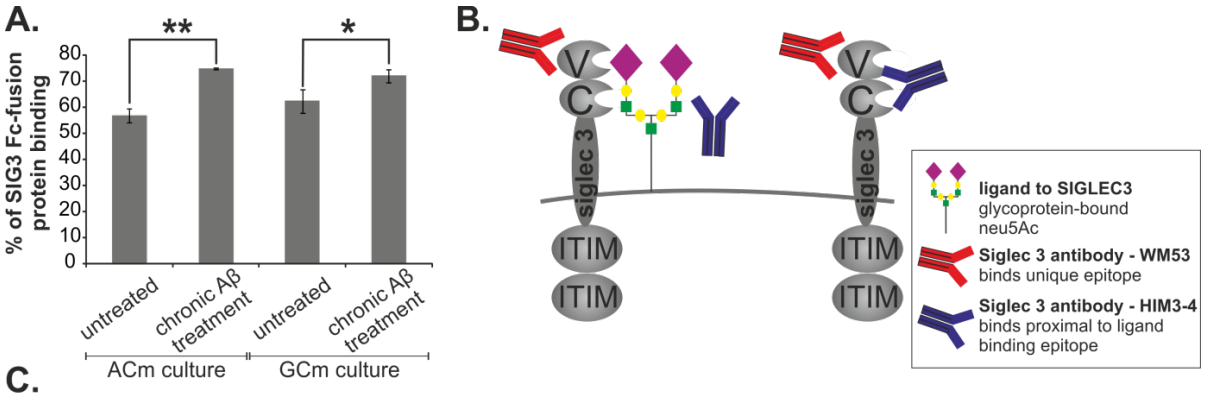

C.

culture condition	treatment	free SIG3 (HIM3-4)	total SIG3 (WM53)	bound SIG3 (WM53-HIM3-4)	bound : total SIG3
SDm	untreated	15.5 ± 2.0	28.2 ± 2.7	12.7 ± 2.5	0.4 ± 0.1
	chronic Aβ treatment	7.8 ± 2.6	38.5 ± 1.1	30.7 ± 3.4	0.8 ± 0.1
ACm	untreated	17.3 ± 5.2	34.3 ± 8.4	17.0 ± 4.5	0.4 ± 0.0
	chronic Aβ treatment	10.2 ± 3.1	37.0 ± 6.2	26.8 ± 4.3	0.7 ± 0.0
GCm	untreated	7.7 ± 2.8	35.4 ± 6.6	27.7 ± 6.4	0.8 ± 0.1
	chronic Aβ treatment	9.8 ± 4.5	30.4 ± 5.8	20.6 ± 1.6	0.7 ± 0.1

Figure 12: SIGLEC3 binds Neu5Gc in *cis* to a higher degree than Neu5Ac. SIGLEC3 can bind to both Neu5Ac (56.8 % ± 2.7 %) and Neu5Gc (62.5 % ± 4.4 %). Under both culture conditions, chronic treatment with Aβ increases SIGLEC3 Fc-fusion protein binding to 75.0 % ± 0.4 % and 72.1 % ± 2.4 %, respectively (A). Of the total SIGLEC3 expressed on the cell surface, roughly half are expected to be ligand-bound to maintain baseline homeostatic inhibitory signaling (representative image, B). The difference between total protein expression of SIGLEC3 (determined by clone WM53 antibody binding) and SIGLEC3 free from ligand-binding (determined by clone HIM3-4 antibody binding) provides the % of SIGLEC3 cis-bound to ligands (C). A ratio of the bound SIGLEC3 to total SIGLEC3 indicates that GCm cultured cells constitutively bind SIGLEC3 to a higher degree than SDm and ACm cultured cells. Similarly, cells chronically treated with Aβ bind SIGLEC3 to a higher degree than untreated cells, irrespective of culture conditions (C; average ± SEM). n=4

Therefore, binding of the HIM3-4 clone would only occur if the protein is free from ligand binding (figure 12B). By calculating the difference between the *total* SIGLEC3 (% of WM53 binding) and the *free* SIGLEC3 (% of HIM3-4 binding), it is possible to identify the percentage of protein bound by ligands (figure 12C). By this logic, it was identified that approximately half of total SIGLEC3 protein expressed is bound in cis with self-ligands (cis-bound/total protein; 0.45 ± 0.06 and 0.45 ± 0.05 under SDm and ACm culture, respectively). Interestingly, cells cultured in GCm showed significantly higher cis-interacting SIGLEC3 (0.78 ± 0.09). Similarly, chronic stimulation of cells with low dosages of Aβ also significantly increased SIGLEC3 cis-binding in SDm and ACm culture (0.79 ± 0.07 and 0.73 ± 0.04, respectively). However, chronic treatment with Aβ under GCm did not further increase the already higher percentage of cis-bound SIGLEC3 (0.72 ± 0.07, figure 11B). In conclusion, around half of the SIGLEC3 expressed is cis-bound to maintain homeostatic inhibition. Additionally, Neu5Gc elicits a comparable increase in cis-bound SIGLEC3 (figure 12C).

In the case of Neu5Gc, its ability to incorporate into the cellular glycocalyx (figure 10) as well as its binding capacity to SIGLEC3 has been confirmed (figure 12A), as described above. In addition to this, there is significantly more binding to SIGLEC3 as compared to ACm and SDm cultures (figure 12B). However, since Neu5Gc is a foreign sialic acid to the human SIGLEC3, the question remains: *does binding of Neu5Gc to SIGLEC3 propagate inhibitory signaling?*

3.4.4 Neu5Gc bound to inhibitory receptor SIGLEC3 does not propagate inhibitory signaling

Western blot analysis revealed reduced recruitment of downstream molecules of the inhibitory pathway, which indicate absence of inhibitory signaling, under GCm culture conditions.

Direct evidence for the absence of inhibitory signaling can be elucidated from the shp1 recruitment to SIGLEC3. SIGLEC3, upon ligand binding, recruits shp1 to further propagate inhibitory signaling. Insufficient shp1 recruitment could be indicative of inadequate SIGLEC3 ligand binding. The efficiency of shp1 recruitment to SIGLEC3 can be measured by co-immunoprecipitation of both proteins (representative image, figure 13A). Under ACm culture, shp1 could be successfully detected on immunoprecipitated SIGLEC3. While there is only a tendency towards a decrease in shp1 recruitment upon chronic treatment with Aβ, GCm cultured cells recruited significantly less shp1 than ACm cultured cells (figure 13B). The significantly lower amounts of shp1 recruited to SIGLEC3 in GCm cultured cells indicate that Neu5Gc binding to SIGLEC3 does not adequately activate SIGLEC3 signaling. Whether the inadequate binding is due to steric hindrance or conformational changes on the side of the protein or ligand, is yet to be determined. Nevertheless, it can be concluded that while Neu5Gc can incorporate into the cell surface glycocayx as well as bind SIGLEC3, the SIGLEC3 inhibitory signaling is not effectively propagated. The absence of signaling by an important homeostatic inhibitory receptor such SIGLEC3 could be hypothesized to cause chronic activation of the cells.

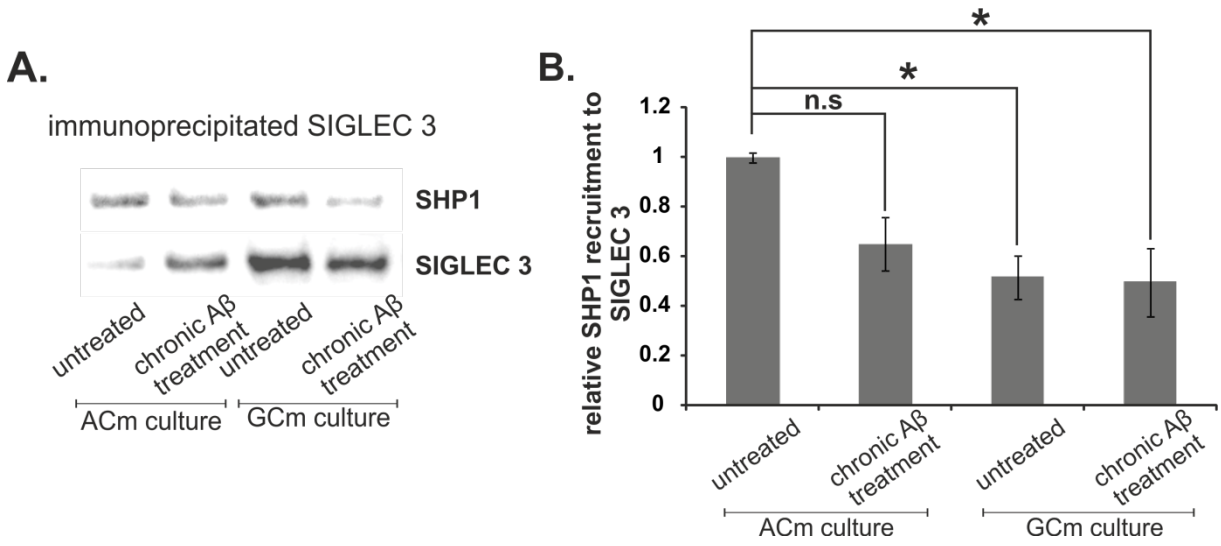

Figure 13: Reduced shp1 recruitment to Neu5Gc-bound SIGLEC3. SHP1 recruitment to SIGLEC3 was obtained by measuring SHP1 antibody stained bands normalized to SIGLEC3 antibody stained bands (A representative image of 4 independent experiments).

Inhibitory signaling through SIGLEC3 is propagated through shp1 recruitment as seen in ACm cultured cells. In comparison, GCm cultured cells recruit significantly less shp1 as seen by western blot analysis. Chronic treatment with Aβ did not influence shp1 recruitment under either culture condition (B). n=4.

3.4.5 SIGLEC3 knockout but not Neu5Gc incorporation during chronic exposure to Aβ downregulates cellular metabolism

MTT analysis revealed that neither the type of sialic acid nor chronic exposure to low concentrations of Aβ affected the metabolic rate. However, the loss of SIGLEC3 signaling significantly reduced cellular metabolism, irrespective of the sialic acid feeding or the Aβ treatment (figure 14). To further elucidate the metabolic status of the cells between the two cell types and under the different conditions, the apoptotic rate was also analyzed by flow cytometry, as described below (section 4.3.6).

3.4.6 Neu5Gc incorporation but not SIG3 KO induces apoptosis

Apoptosis assay was performed to determine whether Neu5Gc incorporation of chronic treatment with Aβ induces programmed cell death. Apoptotic rate of cells was measured by Annexin V staining, using flow cytometry. Annexin V binds phosphatidylserine which is exposed on the cell surface of apoptotic cells.

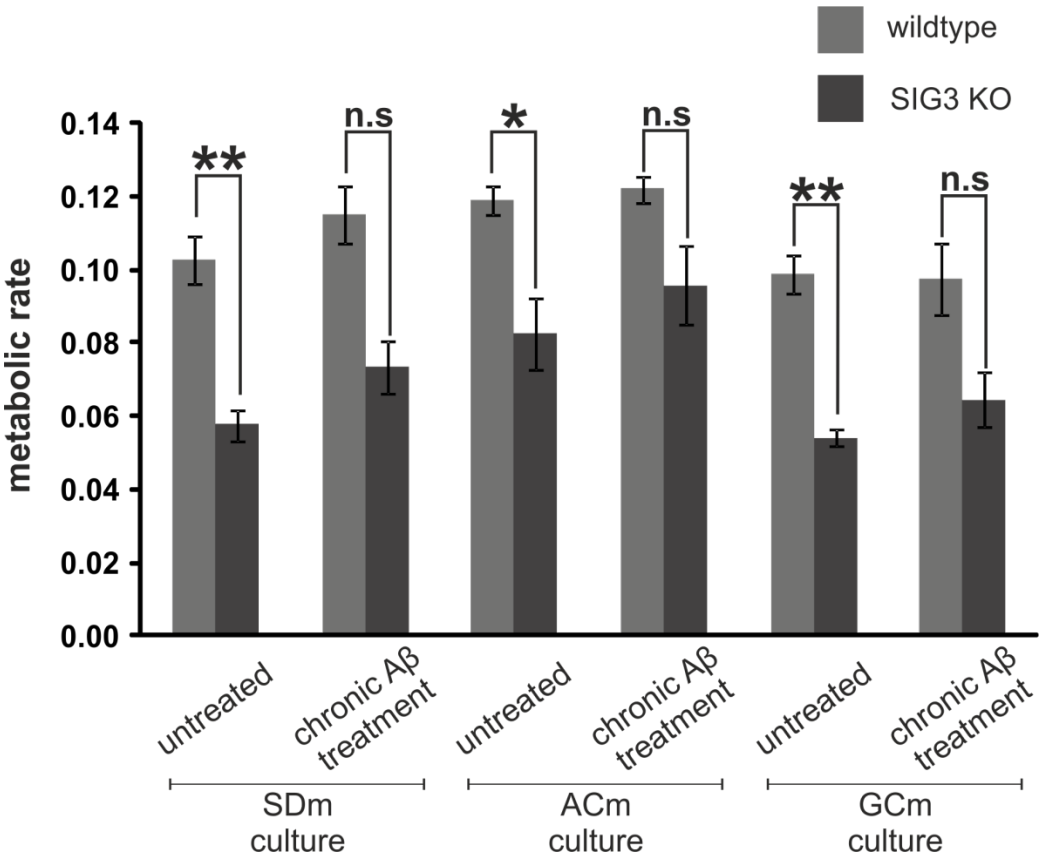

Figure 14: Reduced cellular metabolic activity in SIG3 KO cells. All culture conditions and treatment were comparable within each cell line. Significant differences were only seen between wildtype untreated cells and its corresponding SIG3 KO sample. These differences remained insignificant in the case of chronic Aβ treatment in all cultured conditions n=3.

Therefore, the percentage of apoptosis can be elucidated from the percentage of Annexin V staining. Flow cytometry analysis revealed that GCm cultured cells were significantly more apoptotic than SDm and ACm cultured cells (figure 15). Chronic treatment with Aβ did not influence the apoptotic rate of the cells, irrespective of the culture conditions. In accordance with MTT analysis, SIG3 KO cells were significantly less apoptotic than WT cells under each corresponding culture condition. The lowered apoptotic rate correlates with the lowered metabolic rate of the SIG3 KO cells, in comparison to WT.

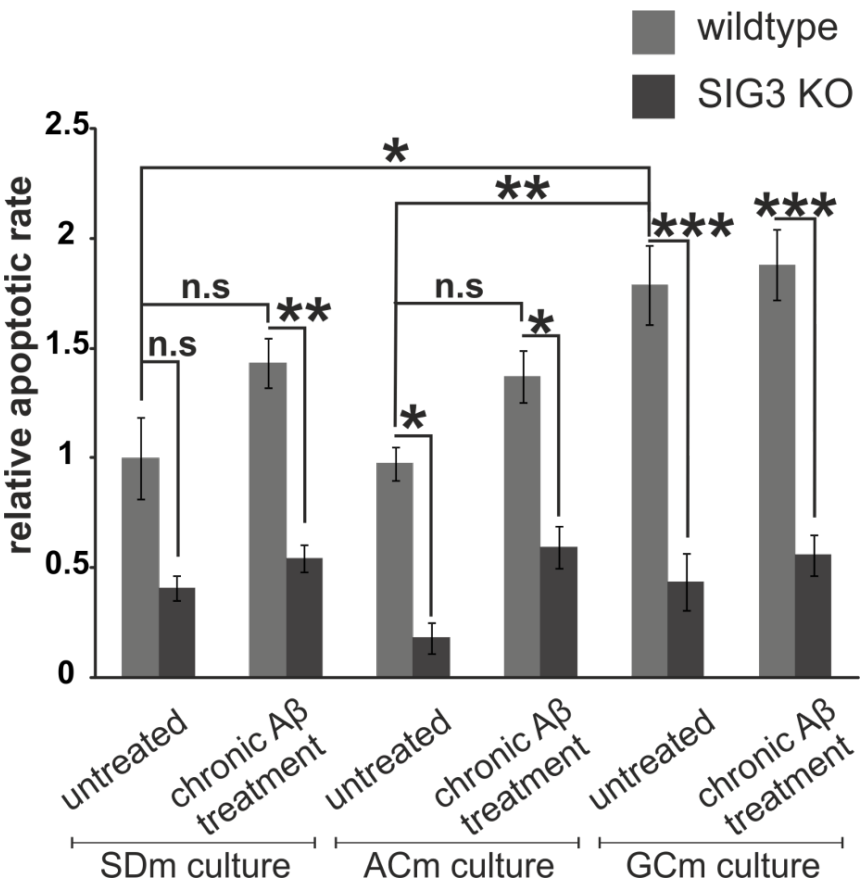

Figure 15: Neu5Gc induces apoptosis. GCm cultured cells were significantly more apoptotic than SDm and ACm cultured cells. Chronic treatment with Aβ did not influence apoptosis. SIG3 KO cells were significantly less apoptotic in comparison to corresponding culture

condition in WT cells, except in SDm untreated cells. Apoptotic rate of SIG3 KO cells remained unchanged, irrespective of sialic-acid feeding and chronic treatment with Aβ. n=3.

3.4.7 Neu5Gc in combination with Aβ treatment induces molecules of activatory pathways

Indirect evidence of absent inhibitory signaling was obtained by detecting the phosphorylation status of the downstream activatory molecule ERK (extracellular signal regulated kinases) at 42 and 44 kDa, normalized to total ERK protein immunoprecipitated (figure 16A). Increase in phosphorylated ERK (pERK) in ratio to total ERK (tERK) indicates increased activation of the cells. THP1 WT cells cultured under GCm conditions showed a tendency towards increased phosphorylated ERK in comparison to ACm cells. However, the GCm induced increase was not significant. Similarly, chronic Aβ exposure in ACm cultured cells was also insufficient to induce significant phosphorylation of ERK. Interestingly, a combination of GCm culture and chronic Aβ exposure significantly up regulated the phosphorylation of ERK. This up regulation was comparable to the increased ERK phosphorylation seen in SIG3 KO cells under all culture conditions (figure 16B).

3.4.8 Neu5Gc incorporation but not SIG3 KO or chronic treatment with Aβ causes radical bursts.

Reactive oxygen species (ROS) production was analyzed to assess the radical production under the different sialic acid feeding conditions. SDm and ACm cultured cells produced comparable amounts of ROS, as measured by DHE staining. In comparison to SDm and ACm cells, GCm cultured cells produced significantly higher quantities of ROS. However, chronic Aβ exposure did not induce ROS production under any culture condition (figure 17).

It is crucial to indicate that while cells chronically exposed to Aβ under SDm and ACm conditions are not in a pro-inflammatory status; phagocytosis could still be induced, as shown in the data below (section 4.3.9). In the case of SIG3 KO cells, absence of inhibitory signaling did not induce ROS production. SIG3 KO cells produced comparable quantities of ROS irrespective of the type of sialic acid feeding and chronic treatment with Aβ. Therefore, Neu5Gc induced ROS production cannot be propagated in the absence of SIGLEC3.

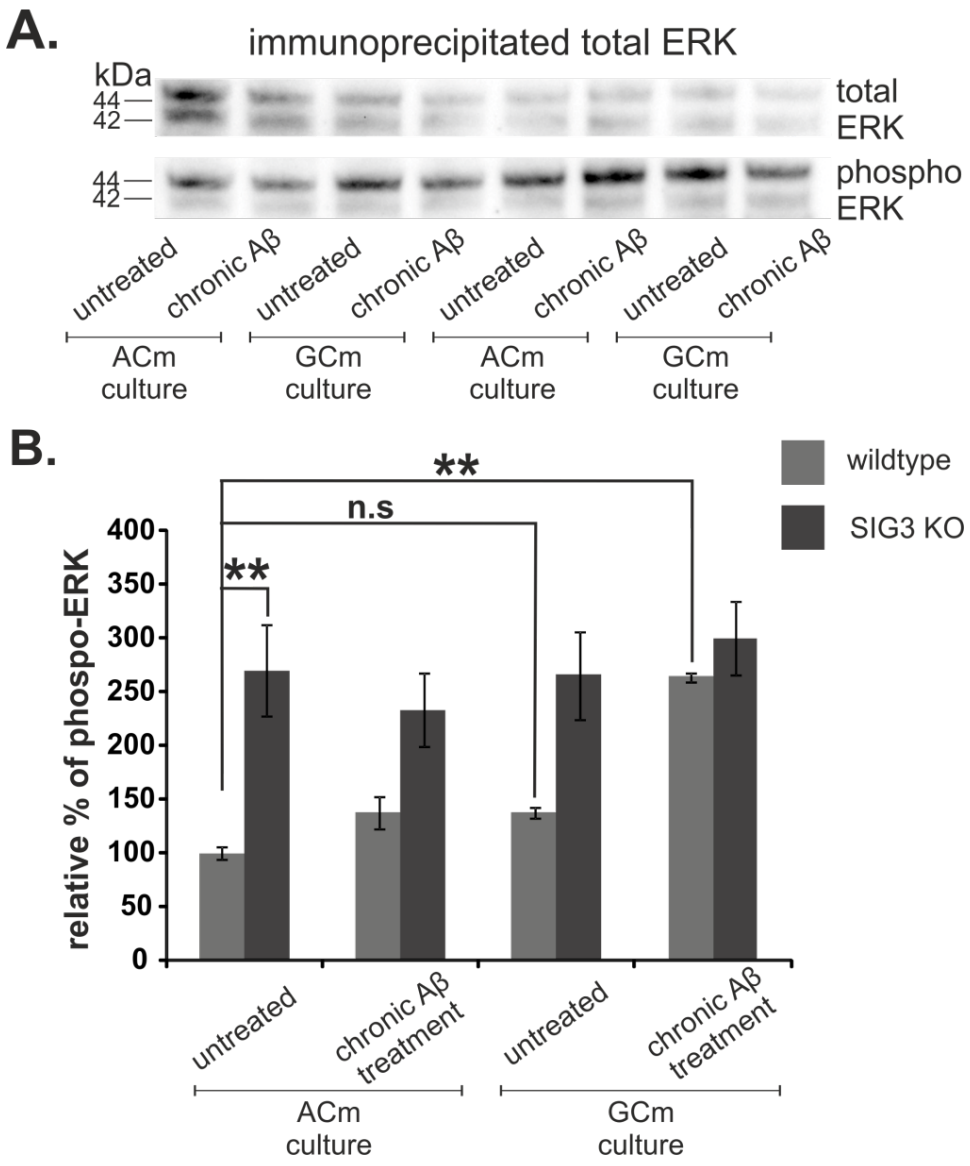

Figure 16: Increased phosphorylated ERK in GCm cultures, only when chronically stimulated with Aβ. Western blot analysis shows significant increase in phosphorylation of activatory molecule ERK, normalized to total ERK for corresponding sample, in GCm cultured cells with chronic Aβ treatment. GCm culture or chronic Aβ culture alone did not elicit a significant increase in phosphorylated ERK. SIG3 KO cells also expressed significantly higher phosphorylated ERK in SDm and ACm compared to corresponding untreated WT cells.n=5.

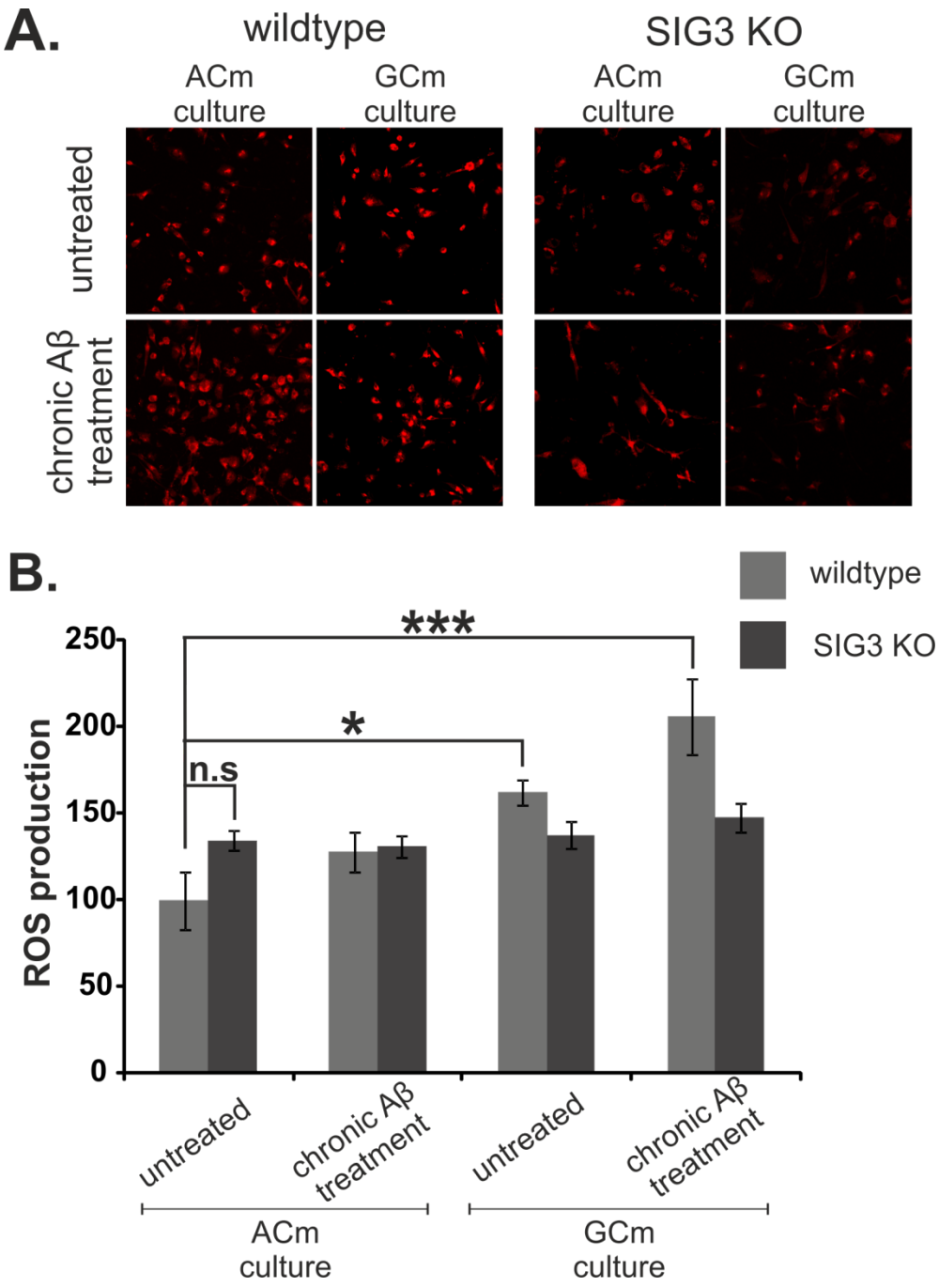

Figure 17: Increased radical production in GCm cultured cells. Representative images of at least five independent experiments, for DHE staining (A). DHE staining analysis revealed an increase in ROS production in GCm cultured WT cells in comparison to SDm and ACm cultured WT cells. Chronic treatment with Aβ showed a slight but insignificant increase in ROS compared to corresponding untreated culture conditions. SIG3 KO remained unchanged, irrespective of culture condition and treatment (B). n= 5-7.

3.4.9 Neu5Gc incorporation, loss of SIGLEC3 or chronic Aβ exposure influence phagocytic capacity of macrophages

Phagocytosis activity was analyzed by measuring the percentage of engulfed biotinylated Aβ (bAβ) after acute treatment. For acute stimulation to measure phagocytosis capacity, bAβ was used as opposed to non-biotinylated Aβ for technical reasons. Biotinylation site of bAβ can be fluorescently labeled with a streptavidin-coupled secondary antibody for detection by confocal microscopy. Data obtained reveals a significant increase in phagocytic capacity of cells in GCm cultured compared to SDm and ACm cultured cells. Additionally, chronic treatment of the cells with Aβ also significantly increased phagocytosis compared to untreated samples under each culture condition (figure 18).

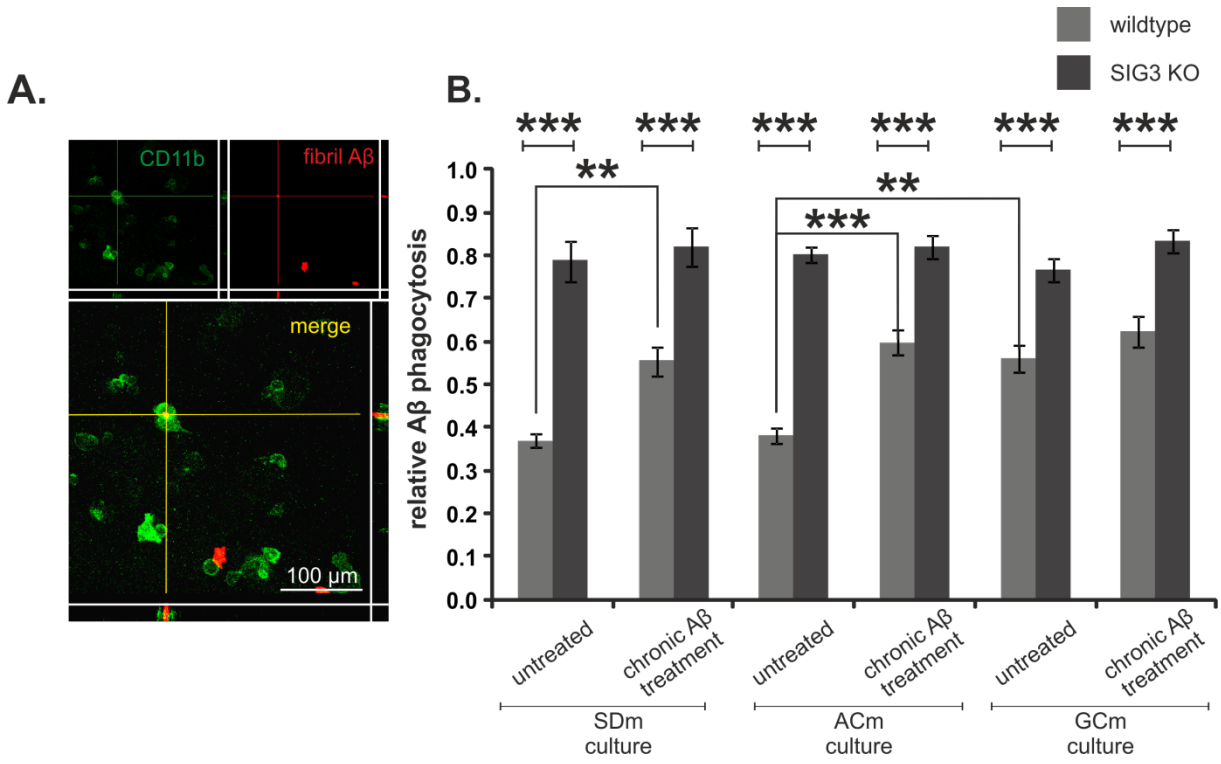

Figure 18: GCm culture as well as chronic treatment with Aβ influence phagocytotic capacity of cells. Representation images of five independent experiments, imaged on x-, y- and z-axis (A). In WT cells, phagocytosis rate under SDm and ACm culture can be increased by chronic treatment with Aβ. GCm cultured cells constitutively phagocytose significantly higher amounts of biotinylated Aβ, compared to SDm and ACm untreated cultures. SIG3 KO cells constitutively phagocytose at a significantly higher rate, irrespective of sialic acid feeding or Aβ treatment, when compared to respective WT cells (B). n=5.

In combination with the ROS production analysis, it can be concluded that increased phagocytosis induced by chronic treatment with Aβ occurs in an anti-inflammatory manner, namely without radical bursts. On the other hand, increased phagocytosis

induced by culturing cells in Neu5Gc containing medium occurs in a pro-inflammatory manner, namely accompanied by radical bursts. SIG3 KO cells constitutively phagocytose significantly higher amounts, when acutely stimulated with Aβ, in comparison to WT cells cultured under the same conditions. Type of sialic acid culture as well as chronic treatment with low concentrations Aβ did not influence the phagocytic capacity of SIG3 KO cells.

3.4.10 Neu5Gc induces transcription of complement cascade molecules

Previous studies have identified an increased activity of classical complement cascade components in LAOD patients. Since induction of the classical complement cascade can modulate phagocytosis, gene transcription of components *c1q* and *c3* were analyzed to determine whether they correlate with the increased phagocytosis seen in GCm cultured cells (section 4.3.9). While gene transcription of *c1q* is exclusively found in the induction of classical complement cascade, transcription of *c3* occurs in all complement cascades (classical, lectin and alternative complement cascades).

Real time PCR analysis revealed increase in transcription of classical complement components exclusively in GCm cultured cells (figure 19). Both components only showed significant differences between ACm and Gcm cultured cells. GCm cultured WT cells transcribed significantly higher amounts of *c1q* and *c3* than ACm cultured WT cells. On the other hand, SIG3 KO cells showed a tendency for reduced transcription of both factors in comparison to WT THP1 cells (figure 19). No significant differences in transcription were observed in SIG3 KO cells among the different culture conditions as well as treatments for *c3* transcription (figure 19A). In the case of *c1q* transcription in SIG3 KO cells, while a tendency for increased transcription was observed after chronic treatment with Aβ, these differences were insignificant (figure 19B).

Therefore, induction of complement cascade molecules correlate with increased phagocytosis seen in GCm cultured cells. To determine whether the increased phagocytosis in GCm cultured cells is indeed mediated through the classical complement pathway, inhibition studies using antibodies blocking complement receptor 3 (CR3) must be performed (preliminary data in section 4). While increased

phagocytosis in GCm cultured cells could be hypothesized to be mediated by the complement cascade, this is not the case for cells chronically treated with Aβ.

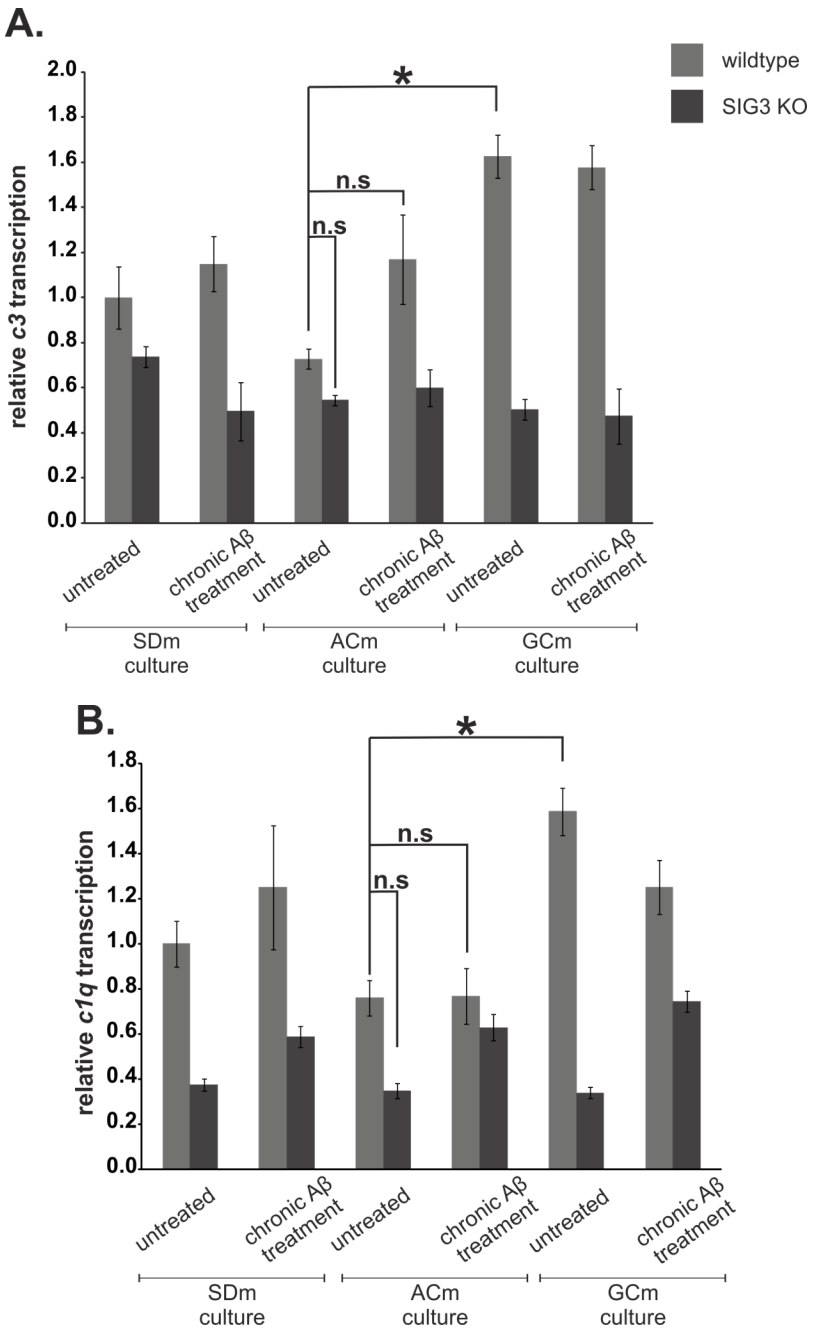

Figure 19: GCm cultured cells significantly increase transcription of complement components. C1q and C3 are components of the classical complement cascade. Both components are significantly increased when cells are cultured in GCm, irrespective of chronic Aβ treatment. SIG3 KO cells tended to transcribe lower levels of both components, however the reduced transcription levels were not significant. (A) n=3-4; (B) n=3-5.

3.4.11 TREM2 expression is induced by chronic treatment with Aβ in WT cells and drastically reduced in SIG3 KO cells.

Increased TREM2 expression has been previously observed in Aβ plaque-associated microglia in LOAD brains. One function of TREM2 signaling includes modulation of phagocytosis. Therefore, expression of TREM2 was studied as a possible mechanism by which phagocytic capacity of cells can be increased upon chronic treatment with Aβ, as seen in section 3.4.9.

In WT cells cultured under SDm or ACm conditions, chronic treatment with Aβ significantly increases TREM2 expression. However, GCm cultured WT cells could not be induced to increase TREM2 protein expression, irrespective of chronic treatment with Aβ. Interestingly, SIG3 KO cells drastically reduced TREM2 expression levels and neither culture conditions nor chronic treatment with Aβ could induce modulation of TREM2 expression.

Therefore, increase in TREM2 expression correlates with increased phagocytosis seen in WT cells chronically treated with Aβ, under SDm and ACm cultures. To determine whether this increased phagocytosis is indeed mediated via TREM2 signaling, inhibition studies using blocking antibody against TREM2 must be performed (preliminary data in section 4). While modulation of phagocytosis observed in WT cells could be hypothesized to be mediated via TREM2, the increased phagocytosis seen in SIG3 KO cells occurs despite significantly reduced TREM2 expression levels. Therefore, the increased phagocytic activity of SIG3 KO cells is mediated by a unique pathway not including TREM2 signaling.

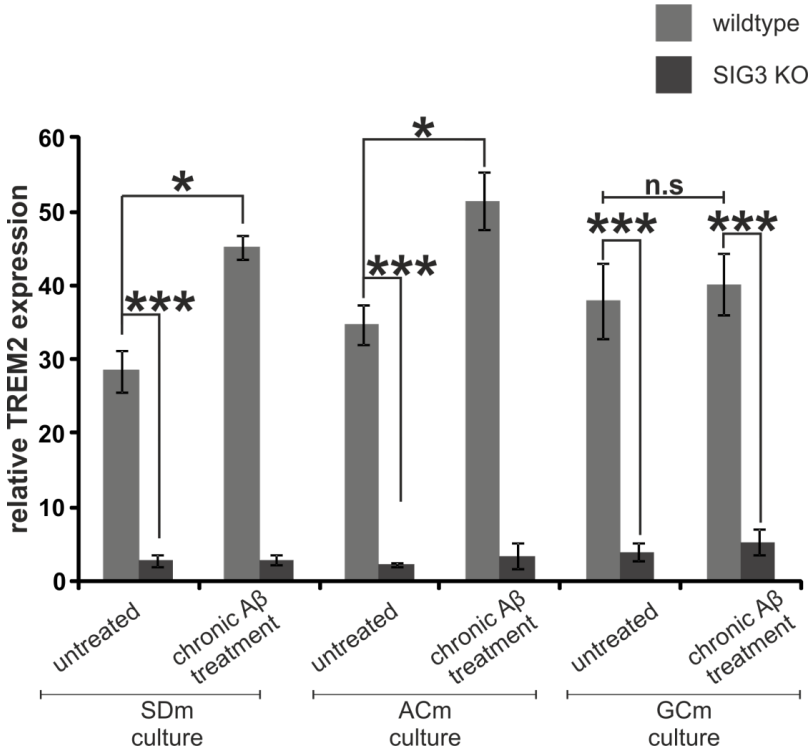

Figure 20: Trem2 protein expression is not inducible in GCm cultured cells and drastically reduced in SIG3 KO cells. TREM2 protein expression was inducible upon chronic treatment with Aβ, when WT cells were cultured in SDm or ACm conditions. However, GCm cultured WT cells were incapable of increasing TREM2 expression, when chronically treated with Aβ. SIG3 KO cells significantly reduced TREM2 expression in comparison to WT in corresponding samples, irrespective of culture conditions or Aβ treatment. n=5.

4. Discussion

Evolution of the modern man began with the first member of the genus Homo over 2.5 million years ago. Over the numerous species ranging from Homo *habilis* to modern man, several crucial evolutionary changes occurred to ensure survival against external factors like climate and predators (Noonan 2010). In addition to physical changes in the skeletal and nervous system, vital changes in the immune system also occurred (Abi-Rached et al. 2011). Around 2 million years ago, one such crucial change occurred exclusively in members of the genus Homo at the molecular level, namely a 92 base pair deletion in exon 6 of the gene *cmah* (Chou et al. 1998)(Varki 2001). The enzyme CMAH is responsible for hydrolyzing acetylated sialic acid (Neu5Ac) to produce glycosylated sialic acid (Neu5Gc). Taken together, the development of a complex CNS as well as a robust immune system led to a thriving species of humans that are continually evolving to this day. The immune system, including phagocytes such as macrophages in PNS and microglia in the CNS are crucial in defending the host against infections. Microglia in the CNS maintain homeostasis and therefore are vital in supporting co-ordinated functioning of the host.

4.1 Functions of microglia and their contribution to LOAD

4.1.1 Microglia in health and disease

Microglia are the only *resident* immune cells of the immune-privileged CNS. Being the primary-response team to protect the CNS, microglia express specialized receptors that are useful in detecting chemical imbalances or changes indicative of various stimuli ranging from dangerous pathogenic invasion to routine synaptic pruning. In the case of the former, microglia are stimulated towards a pro-inflammatory state. Pro-inflammatory status refers to the state at which microglia can effectively proliferate, migrate to site-of-infection and destroy invading pathogens by phagocytosis and radical bursts. Radicals such as reactive oxygen species (ROS) or reactive nitrogen species (RNS), among others, are a necessary by-product of pro-inflammation upon stimuli with pathogen-associated molecular patterns (PAMPs). In addition to destroying pathogens, radical bursts also cause collateral damage to neighbouring host cells. However, production of radicals is often a fast and transient event and therefore collateral damage to host cells is highly localized and limited.

Besides host defense, maintenance of homeostasis by phagocytosing apoptotic cells and synaptic pruning are by far some of the most important responsibilities of microglia (Maderna & Godson 2003)(Tremblay et al. 2010). Synaptic pruning during development as well as in the adult CNS can be mediated by anti-inflammatory phagocytosis without radical damage to neighbouring cells (Michelucci et al. 2009)(Paolicelli et al. 2011)(Bilimoria & Stevens 2015)(Wu et al. 2016). In addition, immune cells in this state can release neuroprotective factors such as BDNF, GDNF and TGFβ. Taken together, microglia perform numerous and complex functions, which are sensitively balanced in order to maintain homeostasis and provide immune defense.

Therefore, an imbalance in the sensitive signaling of microglia can lead to a disproportionate response resulting in chronic inflammation and neurodegeneration (Bradshaw et al. 2013)(Brown & Neher 2014)(Bodea et al. 2014).

In the case of AD, the most obvious pathological features found in post-mortem AD brains are extracellularly accumulated Aβ plaques and intracellularly accumulated tau proteins. However, studies show that AD patients with clinically diagnosed dementia as well as age-matched non-demented controls both have Aβ deposits (Coria et al. 1993)(Esparza et al. 2014). The critical difference between AD patients and control individuals lie with the plaque morphology/density and their associated glial cells. Post-mortem studies show that an AD brain has a higher plaque coverage and severe microgliosis and astrogliosis proximal to plaques, in comparison to a non-demented brain (Esparza et al. 2014). For this reason, the molecular environment in a pre-clinical AD brain must be intensively studied to identify the initial source of inflammation. Decades before cognitive deficits begin to manifest in an AD patient, molecular events occur, that distinguish a potential AD brain from non-demented control. One such event is the upregulation of the classical complement pathway (Hong et al. 2016)(reviewed by Tosto & Reitz 2013). This association is further substantiated by genome-wide association studies (GWAS) that have identified complement receptor 1 (CR1) as a risk factor for LOAD (Hollingworth et al. 2011)(reviewed by Tosto & Reitz 2013).

In addition, inflammation is also found in early stages of LOAD. Microglia are considered as one of the primary sources of inflammation in the CNS (Streit 2004)(Ridolfi et al. 2013)(reviewed by Doens et al. 2014)(Malik et al. 2015).

4.1.2 Inflammation in LOAD

Neuroinflammation is widely accepted as the cause leading to degeneration of neurons. Microgliosis has been found to be a pathological feature of AD, along with Aβ plaques (Solito & Sastre 2012)(Herber et al. 2007). However, studies which indicate that Aβ can induce inflammation should be critically viewed due to the technicalities behind the experimental setups. On the one hand, several studies load high quantities, above biological levels, of fibrillary Aβ to elicit a pro-inflammatory stimuli (Milton et al. 2008)(Parajuli et al. 2013). On the other hand, several studies use cellular or animal models that do not fully represent the array of human specific receptors or ligands (Milton et al. 2008)(Parajuli et al. 2013)(Chin 2011). Therefore, attention must be paid to the experimental setup as well as model system used to study the source of inflammation that exacerbates LOAD pathology.

The typical microglial characteristic functions were studied in this thesis to elucidate the possible pathways that lead to pre-clinical inflammation. To fully understand the microenvironment of microglial cells, their receptors and ligands must be taken into account. One feature that is unique to human cells are their sialic acid composition.

4.2 Sialic acids and SIGLECs

A single sialic acid molecule, termed by the swedish biochemist Gunnar Blix in 1952 (Blix et al. 1952), is a glycan monomer in its most basic form. Although small and seemingly irrelevant, sialic acids are vital molecules with several functions among all eukaryotes (Varki & Gagneux 2012)(Rachmilewitz 2010). Mammalian cells utilize the sialic acids in their multifarious combinations and conformations to communicate and maintain homeostasis. Studies have attributed reduced neurotoxicity by radicals and increased life span to sialic acids and their binding to receptors (Claude et al. 2013; Schwarz, Pearce, et al. 2015)(Schwarz, Springer, et al. 2015). This sensitive signaling through sialic acids has been hijacked by pathogens to evade host immune response upon infection by molecular mimicry (Doxey & McConkey 2013). Sialic acids and their receptors are perenially in an evolutionary race to overcome pathogen mimicry and improve upon host immune defence (Wang et al. 2012)(Padler-Karavani, Tremoulet, et al. 2013). Protection against zoonotic diseases has been hypothesized as one of the main criteria for the loss of CMAH enzyme functionality specifically in humans (reviewed by Varki 2001).

The loss of Neu5Gc as a native ligand to human sialic-acid binding receptors led to a desensitization of these receptors to Neu5Gc and a preference towards Neu5Ac (Blixt et al. 2003)(Padler-Karavani, Hurtado-Ziola, et al. 2013). One such family of sialic acid binding receptors include SIGLECs. The majority of SIGLECs, called CD33-related SIGLECs, are rapidly evolving and differ from species to species. One clear example of species differences among CD33-related SIGLECs can be seen in the receptor SIGLEC3. Human SIGLEC3 (hSIGLEC3) carries two intracellular tyrosine-based inhibitory motifs. The tyrosine-based inhibitory motifs (ITIM and ITIM-like), by which hSIGLEC3 signals, can propagate an inhibitory signaling cascade which modulates activatory signaling pathways. On the other hand, mouse SIGLEC3 (mSIGLEC3) carries a single ITIM-like domain intracellularly and additionally carreis a positively charged residue in the transmembrane region. The positively charged residue is a putative association site for the activatory protein DAP12. Therefore, it can be assumed that mSIGLEC3 could propagate activatory signaling pathways (Crocker et al. 2007). This high variability in the family of SIGLECs among mammals hints at the sensitivity towards and complexity of their preferential ligands, namely sialic acids (Padler-Karavani et al. 2014).

Although humans are incapable of producing Neu5Gc from Neu5Ac, several studies have shown trace evidence of Neu5Gc found in human cancer tissue and fetal tissue as well as antibodies against Neu5Gc in the blood stream (Malykh et al. 2001)(Tangvoranuntakul et al. 2003)(Hedlund et al. 2007). However, the non-human immunogenic sialic acid elicits an immune reaction in response to Neu5Gc, called xenosialitis (Bergfeld et al. 2012)(Samraj et al. 2015). Xenosialitis leads to inflammation and exacerbation of vascular pathology.

The source of immunogenic Neu5Gc in human tissue was found to be metabolic incorporation from diet (Bardor et al. 2005)(figure 6). Once exposed on the cellular glycocalyx, sialic acids are available as ligands to sialic acid binding receptors. Futhermore, due to the desensitization of the human system to Neu5Gc, this sialic acid is rather resistent to enzymatic turnover by human sialidases, leading to an accumulation on cells when a persistent source is available (Taguchi et al. 2015)(Davies et al. 2012). Therefore, Neu5Gc could be hypothesized to disrupt cellular homeostasis. This possibility is of interest with respect to LOAD for two reasons; first, Neu5Gc has been proven to elicit an immune response and therefore

cause inflammation (Samraj et al. 2015). Second, sialic acids including Neu5Ac and Neu5Gc are ligands to the inhibitory receptor SIGLEC3. Polymorphisms of SIGLEC3 have been associated to LOAD by GWAS (Hollingworth et al. 2011). Furthermore, while xenosialitis has been implicated in cancer progression (Malykh et al. 2001)(Samraj et al. 2015), autoimmune hypothyridism (Eleftheriou et al. 2014) and infertility (Ma et al. 2016), the inflammatory response to Neu5Gc in the brain - particularly in terms of neurodegenerative diseases remains unresolved.

4.3 Microglial cells as a human model system to study xenosialitis in LOAD

Since extensive species differences exist, this report primarily aims at maintaining a “human-like” culture model. Cells were cultured in either serum-deficient medium (SDm) or Neu5Ac-supplemented medium (Acm) as controls which represent a human native sialic acid environment. In parallel, cells were treated with Neu5Gc-supplemented medium (GCm), to study the influence of Neu5Gc incorporation on immune cell functions. Finally, to mimic the early environment preceding clinically confirmed AD, cells were chronically exposed to nanomolar concentrations of Aβ. The concentration of Aβ used for chronic treatment was intentially chosen to be dramatically lower than typically used in studies with regards to AD research. Previous studies which describe an inflammatory response from immune cells in response to Aβ use concentrations of 2.5 µM (Milton et al. 2008), 5 µM (Parajuli et al. 2013) and above. However, early in disease onset, Aβ is not present as highly concentrated wide-spread plaques but rather deposited as puncta in the form of monomers or oligomers (Hong et al. 2016).

4.3.1 Microglial cells as a human model system

The first aim of this project was to establish a stable and proliferative human microglial cell line as a human specific model system cultured in serum-free medium. To this end, human induced pluripotent stem (iPS) cells were differentiated into a microglial cell line (SdMic1 and SdMic2). However, the obtained lines proved to be genetically instable. Karyotyping studies indicated that the microglial lines carried increased chromosomal numbers in comparison to the iPS cells from which they were generated. Further analysis with techniques such as fluorescence in situ hybridization (FISH) could help identify the specific chromosomes that have been

duplicated. Although the discrepancies in chromosomes were not specifically identified, previous publications have also described instabilities in iPS cultures and their derivatives (Mayshar et al. 2010)(Varela et al. 2012). Further confirmation of genetic instability of SdMic lines was observed from SNP analysis. The abberent reads can be attributed to the increased chromosomal numbers of the cell lines. Therefore, while the SdMic lines were proliferative and could be easily expanded for molecular studies, the genetic instability made them an inadequate model system. In order to obtain genetically stable microglial cells, optimizations to the previously described protocol were made by including quality controls such as routine in-house STR analysis runs (Cooper et al. 2007). Further optimizations included culturing stem cells on a matrix layer and screening for $KDR^{+}CD235a^{+}$ population in the embryonic body (EB) stage. The percentage of double positive cells represents the embryonic hematopoiesis population which is known to give rise exclusively to microglial cells of the CNS (Ginhoux et al. 2010). In addition, stimulation of myeloid progenitors and microglial precursors by IL34 and MCSF aimed at supporting their development. The obtained microglial cells (iPSdM9) were positively indentified as microglia by their heritage (namely $KDR^{+}CD235a^{+}$ population) and the expression of typical markers such as IBA-1, CD11b and TREM2. Of all the cells identified by DAPI staining, only a modest population was positive for the above mentioned markers. This non-homogenous population is due to the low microglial cell numbers obtained in the differentiation plates. The few thousand microglia harvested were manually picked using a micropipette and therefore other cells types besides microglia were also present. Since the microglia are not highly proliferative, they do not easily overgrow the other cell types to develop a homogenous cell line. Further optimization is required to obtain higher quantities of microglia that could represent an *in vitro* human model system, sufficient for molecular studies. Limitations of low cell numbers can be overcome by upscaling the differentiation, however, efficiency of differentiation could be bettered by increasing the proportion of $KDR^{+}CD235a^{+}$ population in the EB stage, for example by activating wnt pathway. While direct differentiation from stem cells to microglial cells is the most efficient option, the disadvantage includes the absence of neural input during microglial maturity that occurs *in vivo*. By including an EB development stage, both neural and myeloid progenitors develop in the same environment. Neuronal and astrocyte cell types are found in the differentiation plate alongside microglial cells. The cross-talk between

microglia and its neighboring neural cell types can provide vital signals to mature microglial cells. Finally, increased stimulation of colony stimulation factor receptor is a potential target to improve microglial proliferation.

4.3.2 Influence of Neu5Gc on immune cell functions

Validation of experimental setup

Due to limitations in cell numbers of iPSdM9 microglial cells, THP1 monocyte-derived macrophages were substituted as a human model system to study the influence of incorporated Neu5Gc on immune cell functions in general, and SIGLEC3 signaling in particular. THP1 cells express surface markers typically found in both microglia and macrophages and well represents the human species specific immune cell type. The capability of human cells to metabolically incorporate Neu5Gc has been previously shown by publications and was further confirmed in this thesis (Tangvoranuntakul et al. 2003)(Bardor et al. 2005). Presence of Neu5Gc on the cell surface after culturing in GCm was confirmed by flow cytometry analysis using a specific anti-Neu5Gc antibody. Furthermore, chronic treatment of cells with Aβ significantly increased the detection of Neu5Gc on the cell surface. This indicates that the Aβ treatment was identified by the immune cells, which respond by increasing the sialic acids on the cell surface. Of the total Neu5Gc incorporated, xCGE-LIF identified that around 1 % was present in the form of glycoproteins (section 3.4.1). Therefore, it can be assumed that the majority of Neu5Gc is present in the form of glycolipids. The fact the sialic acids are primarily found onon glycolipids has been previously described by Schnaar and colleagues (Schnaar et al. 2014). Nevertheless, Neu5Gc isolated from glycolipids must also be measured by xCGE-LIF for confirmation. The incorporated Neu5Gc was shown to cause wide-scale dysregulation of several immune processes. RNA sequencing identified that over 1400 genes were differentially expressed in GCm cultured cells in combined comparison to SDm and ACm cultured cells. Interestingly, the pathways that were highlighted as being dysregulated include cell signaling, regulation of immune responses, regulation of response to stimuli and migration (section 3.4.2). This dysregulation found in GCm cultured immune cells indicates a proinflammatory phenotype, which is appreciable when compared to studies describing xenosialitis caused by Neu5Gc.

RNA sequencing established that Neu5Gc incorporation pushed immune cells towards a proinflammatory phenotype. Therefore, the question arose; *Which*

pathways mediate the negative effects of Neu5Gc? Since Neu5Gc is a monosialic acid, the sialic acid binding receptor SIGLEC3 came into focus. Most interestingly, polymorphisms of SIGLEC3 have been associated with LOAD. Although Neu5Gc is no longer a native human sialic acid, SIGLEC3 can bind Neu5Gc (Blixt et al. 2003). The capacity of SIGLEC3 to bind Neu5Gc was further confirmed in this thesis by flow cytometry analysis using SIGLEC3 Fc-fusion protein. SIGLEC3 Fc-fusion protein could bind both ACm and GCm cultured cells to the same extent. Binding of the Fc-fusion protein was futher increased when the cells were chronically treated with Aβ, in both ACm and GCm culture conditions (section 3.4.3). This data correlates well with the increased Neu5Gc detection in cells chronically treated with Aβ, in comparison to control cells (section 3.4.1). Therefore, an increase in ligands on the cell surface leads to an increase in protein binding.

Influence of Neu5Gc on SIGLEC3 signaling

Inhibitory receptors of the SIGLEC family and their downstream signaling are important in maintaining homeostasis (Johnson et al. 2013)(reviewed by Linnartz et al. 2010). SIGLECs are known to bind sialic acids on their own cell surface by means of so-called *cis* interactions (Crocker et al. 2007). SIGLECs bound in *cis* maintain homeostasis by propagating a baseline inhibition signal. In this thesis, the percentage of *cis* interacting SIGLEC3 was identified by taking advantage of the various SIGLEC3 antibodies available. Two clones of SIGLEC3 antibodies bind at two different epitopes; clone WM53 binds at a unique epitope that is not obstructed irrespective of ligand binding to SIGLEC3 and HIM3-4 clone binds an epitope that is proximal to ligand-binding epitope and therefore, can only bind if the protein is not ligand bound. Therefore, the clone WM53 determines the total SIGLEC3 while the clone HIM3-4 determines unbound / free SIGLEC3. By subtracting the total SIGLEC3 from free SIGLEC3 (WM53 - HIM3-4), the percentage of cells with *cis*-interacting SIGLEC3 can be calculated. For further detail, the ratio between bound to total SIGLEC3 was calculated. Increase of SIGLEC3 bound to ligand would indicate an increase in inhibitory signaling. While SDm and ACm cultured untreated cells exhibited comparable ratios of *cis*-bound SIGLEC, these ratios significantly increased in both cases when chronically treated with Aβ (section 3.4.3). An increase in inhibitory signaling upon Aβ treatment could indicate an attempt to modulate the activation of the cell upon stimulation. GCm cultured cells constitutively exhibited

more bound SIGLEC3, which was not further increased upon binding to Aβ (section 3.4.3). By similar logic, the cells could also be increasing SIGLEC3 signaling to modulate cellular activation. However, in the case of GCm cultured cells, two more possibilities should be taken into consideration. First, since human sialidases are incapable of efficiently turning over Neu5Gc, the SIGLEC3 could simply be persistently bound due to the continual presence of the sialic acid. Since Neu5Gc-bound SIGLEC3 does not propagate inhibitory signaling (section 3.4.4), the second possibility could be an increase in SIGLEC3 binding to compensate for the lack of downstream SIGLEC3 signaling by the inappropriate binding of Neu5GC.

Downstream signaling of SIGLEC3 was determined by the recruitment of SHP1 to the protein. Co-immunoprecipitation of SIGLEC3 and SHP1 determined that significantly less SHP1 was recruited in the case of GCm cultured cells (section 3.4.4). Insufficient recruitment of SHP1 indicates that SIGLEC3 inhibitory signaling is not propagated when Neu5Gc is incorporated. In conclusion, SIGLEC3 Fc-fusion protein analysis confirms that Neu5Gc can bind SIGLEC3 but western blot analysis determines that this binding does not propagate an inhibitory signaling due to a reduced recuitment of the downstream molecule, SHP1.

Upon identification of dysregulated SIGLEC3 signaling due to Neu5Gc, a SIGLEC3 knockout (SIG3 KO) cell line was introduced as a control in comparison to wildtype (WT) cells. Differences observed between ACm cultured WT cells and GCm cultured WT cells could be compared to the respective SIG3 KO cells to determine whether presence of SIGLEC3 attenuates or exacerbates these differences.

Influence of Neu5Gc on functional characteristics of macrophages

First, all samples were tested for their metabolic activity by MTT assay. The metabolic rate was not altered within the cell type, among the different culture and treatment conditions. However, cells of each SIG3 KO culture condition exhibited significantly less metabolism than their corresponding WT samples (section 3.4.5). The fact that the metabolism was also decreased in the control culture conditions, in SIG3 KO cells compared to WT cells, indicates a genotype specific connection. SIG3 KO cells could be downregulating metabolic processes as a compensation mechanism to the loss of an important homeostatic inhibitory signaling pathway.

However, analysis by RNA sequencing are required for further insights to the activatory status of the SIG3 KO cells.

Functional read outs studied in the two cell lines (WT and SIG3 KO), under the different culture conditions (table 1) included apoptosis assay, phosphorylation of ERK, production of ROS, phagocytosis assay, quantitative real time PCR for complement components and surface marker analysis of LOAD-associated TREM2.

In confirmation with RNA sequencing analysis, all functional read outs indicated that GCm cultured cells were more activated than control cells. Incorporation of Neu5Gc in WT cells significantly increased apoptosis, while chronic treatment with Aβ tended to increase apoptosis rate, this tendency remained insignificant. Most interestingly, SIG3 KO cells did not modulate their apoptosis rates, irrespective of culture conditions and treatments. Therefore, knockout out SIGLEC3 rescues the cells from Neu5Gc induced apoptosis (section 3.4.6). An indirect measurement of SIGLEC3 signaling was obtained by detecting the phosphorylation status of downstream activatory molecule, ERK. ERK phosphorylation indicates propagation of an activatory signal. Although, it must be noted that several activation pathways can lead to activatory signaling. However, ERK is a strong candidate downstream of the activatory pathway that could be modulated by SHP1 of the SIGLEC3 inhibitory pathway (figure 4). Chronic treatment of ACm cultured WT cells was not sufficient to increase ERK phosphorylation. Similarly, GCm culture of WT cells in untreated condition was also insufficient for inducing phosphorylation of ERK. However, a combination of GCm culture and chronic treatment with Aβ significantly increased the phosphorylation of ERK in WT cells. In the case of SIG3 KO cells, phosphorylated ERK was constitutively increased in ACm cultured cells (section 3.4.7). Since loss of SIGLEC3 signaling elicits an increase in ERK phosphorylation, this outcome further supports the statement above, which claims that ERK is a strong candidate that can be modulated via SIGLEC3 signaling. As seen in apoptosis assay, phosphorylation of ERK could also not be modulated by culture conditions or treatments in SIG3 KO cells. While the differences between GCm WT and GCm SIG3 KO cells were not significant, a significant difference in ACm culture condition was seen. One of the most critical read outs is the measurement for the production of ROS. Production of ROS is toxic to cells and chronic production can cause wide-spread cellular damage and ultimately neurodegeneration. Fitting with the activated status of GCm cultured

WT cells, Neu5Gc incorporation significantly increased ROS production in comparison to ACm cultured WT cells. Most interestingly, chronic treatement with Aβ in ACm cultured WT cells did not induce an increase in ROS production. This data is in contrast to several publications which utilise high concentrations of fibrillary Aβ to elicit a proinflammatory response. In this thesis, the concentration of Aβ that has been used was intentially chosen to be minimal, yet chronic. Although chronic treatment in this sample did not elicit increased ROS, cells were nevertheless stimulated to upregulate phagocytosis upon stimulation (as further described below and in section 3.4.9), which indicates an appropriate immune response. Chronic treatment in GCm cultured WT cells produced comparable quatities of ROS as untreated cells under the same condition. The SIG3 KO cells were once again stable in ROS production across all culture conditions and treatments (section 3.4.8). Therefore, loss of SIGLEC3 signaling attenuated the detrimental effects of Neu5Gc incorporation. Although chronic treatment of ACm cultured WT cells did not increase the production of ROS, this does not indicate that the cells cannot be activated upon stimulation. On the contrary, acute stimulation of cells with high concentrations of Aβ did elicit a phagocytic response. This increase in phagocytosis occurs in an anti-inflammatory manner, namely in the absence of ROS. Only the WT cells cultured in GCm were phagocytic in a proinflammatory manner and acute stimulation with high quantities of Aβ did not induce an increase in phagocytosis. The inability of GCm cultured WT cells to appropriately respond to stimulation, along with the consititutively high production of ROS further confirms the detrimental effects of Neu5Gc incorporation. Interestingly, the benefits of the lack of SIGLEC3 signaling was furthered by their consitutively high phagocytosis capacity. Interestingly, SIG3 KO cells were significantly more phagocytic than WT cells under any culture condition or treatment (section 3.4.9). The high phagocytosis capacity of SIG3 KO cells, along with their capacity to inhibit ROS production in the presence of Neu5Gc, speaks volumes for the beneficial effects of knocking out SIGLEC3 signaling to attentuate its association with AD risk.

Phagocytosis is an important function of immune cells that is lacking in LOAD and chronic activation is a feature that is in excess. Increased activity of the classical complement cascade has been previously identified in models for AD. Therefore, the influence of Neu5Gc on components of the classical complement pathways came into focus. To this end, quantitative real time PCR analysis of the complement

components c1q and c3 were carried out. C1q is the initiator component of, and exclusive to the classical complement cascade. On the other hand, C3 is a central component upon which the classical, the lectin as well as the alternative complement cascades merge. Transcriptions of both C1q as well as C3 were significantly increased in GCm cultured WT cells, in comparison to ACm cultured WT cells. SDm cultured WT cells tended to be comparable to ACm cultured WT cells albeit without significant differences. Therefore, Neu5Gc could be interpreted as stimulation for the classical complement pathway in LOAD. The SIG3 KO cells tended to transcribe lower quantities of both c1q and c3 components than WT cells of the corresponding culture condition and treatment. Nevertheless, as seen before, Neu5Gc could not induce an increase in c1q or c3 transcription in SIG3 KO cells (section 3.4.10). Chronic treatment with Aβ did not induce significant differences in either cell line or culture conditions. However, chronic treatment with Aβ exclusively modulated the next read out, namely TREM2 surface marker expression. Modulation of TREM2 surface marker expression has been extensively studied with respect to Aβ plaques and by association to LOAD. TREM2 is of particular interest since downstream signaling of TREM2 mediates phagocytosis (figure 4). Microglial cells that are proximal to plaques notoriously upregulate TREM2 expression although the cells are not phagocytically active enough to clear away the Aβ plaques. Conversely, microglia distal to plaques have less TREM2 expression on the cell surface. Several publications emphasize on the importance of functional TREM2 to cope with Aβ plaque clearance in LOAD (Wang et al. 2015)(Yeh et al. 2016). Furthermore, GWAS have associated mutations in TREM2 with increased LOAD risk (Guerreiro et al. 2013). Most interestingly, a recent paper by Chan and colleagues have identified that SIGLEC3 can modulate TREM2 expression (Chan et al. 2015a), which can be critical considering the dysregulation of SIGLEC3 signaling in the presence of Neu5Gc. In this thesis, TREM2 surface marker expression was found to be significantly upregulated in SDm and ACm cultured WT cells, only when chronically treated with Aβ. On the other hand, WT cells cultured in GCm could not increase TREM2 expression upon chronic treatment with Aβ. The incapability to respond to the presence of Aβ further confirms the dysregulated immune cell response to stimuli in the presence of Neu5Gc. The positive correlation between SIGLEC3 and TREM2 (Chan et al. 2015b) was confirmed by the significantly lower expression of TREM2 in all SIG3 KO culture and treatment conditions (section 3.4.11). While knocking out

SIGLEC3 proved to be beneficial in all read outs described above, the drastic reduction in TREM2 could be a critical point to consider when developing therapies.

4.4 A hypothesis on the associations between LOAD incidence, xenosialitis and SIGLEC3

Based on the cummulative results described above, I present a hypothesis that aims at explaining the influence of xenosialitis and SIGLEC3 signaling on LOAD incidence. Studies supported by the World Health Organization (WHO) show a clear tendency towards increased LOAD deaths in populations of industralized countries over populations in the asian and african continents (www.worldlifeexpectancy.com). Data obtained were appropriately standardized to age, and therefore improvements in health care and increased life expectancy have not artifically influenced this data. One major difference among the various nations is diet. Studies show that following a mediterranean diet decreases LOAD risk (as reviewed by (Lin & Scott 2012)), however, a western diet causes chronic glial activation (Graham et al. 2016). Glial activation leading to chronic inflammation is a well documented feature of LOAD (Lull & Block 2011)(Doens et al. 2014). A western diet is defined as being rich in red meat and milk products and is a source of xenosialitis-inducing Neu5Gc sialic acids (Philpott, Tom (April 5, 2011). "The American diet in one chart, with lots of fats and sugars". *Industrial Agriculture*. Grist. Retrieved December 1, 2011.). Therefore, this hypothesis suggests that western diet driven xenosialitis causes inflammation in general, and dysfunctional SIGLEC3 signaling in particular, to increase LOAD risk. LOAD risk is only higher in caucasian populations expressing full length SIGLEC3. This data reiterates the fact that full length SIGLEC3 only exacerbates LOAD in western diet environment, which is a source of Neu5Gc. Since asians and africans do not follow a strict western diet, the dietary supply of Neu5Gc is low and inconsistent. SIGLEC3 variants can either be beneficial or detrimental depending on the populations in which they are expressed. There are two isoforms of SIGLEC3; full length isoform, like the name mentions is the long version of SIGLEC3 as previously described in this thesis, and exon2 spliced isoform which lacks the sialic acid binding domain (Hernández-Caselles et al. 2006)(Malik et al. 2013). Therefore, exon2 spliced SIGLEC3 cannot mediate inhibitory signaling. Interestingly, the well documented risk allele of SIGLEC3 leads to transcription ratios of 9:1 in favor of full length SIGLEC3 isoform. On the other hand, the so-called protective allele modifies the ratio of

expression of SIGLEC3 isoforms full length and exon2 spliced to 7:3, respectively (Schwarz, Springer, et al. 2015). In conclusion, the expression of a functional full length version of SIGLEC3 at a higher degree is detrimental in comparison to exon2 spliced SIGLEC3. Researchers in the field interpret this outcome as follows - loss or reduction of SIGLEC3 signaling causes increased phagocytic removal of Aβ and ultimately lowers LOAD risk (as reviewed by (Angata 2014)). Intriguingly, the overall expression of full length SIGLEC3 is higher in humans than in our closest relatives, chimpanzees and bonobos. This upregulation of the homeostatic receptor is unique to the members of the genus Homo. In addition, the protective SIGLEC3 allele is uniquely found only in modern humans, being absent in our ancestors of the same genus (Schwarz, Springer, et al. 2015). Therefore, the onset of SIGLEC3 protective allele is a rather recent event that arose out of necessity. The incidence of protective allele is highest in the Caucasian populations that consume western diet (figure 21) and is least prevalent in Asian and African populations. Therefore, the association between western diet derived Neu5Gc detrimentally affecting SIGLEC3 signaling to increase LOAD risk could have been the eminent trigger that supported the emergence of the protective allele of SIGLEC3.

In conclusion, the inflammatory effects of Neu5Gc, which is already linked to cancer progression, could also be the initiator of chronic activation and dysregulated immune responses in microglial cells. The malfunctioning inhibitory SIGLEC3 may further exacerbate disease progression leading to imbalances in homeostasis and a persistent pathological environment. Malfunctioning microglia cannot respond to stimuli such as Aβ, which accumulate into plaques when left unchecked (figure 22). Understanding the role of all components from a molecular level to a pandemic level is crucial for the development of therapies that would hinder disease progression, outside of genetic susceptibilities. On a final note, all data point towards the benefits of a diet low in red meat and milk products. Such a dietary recommendation is already in place as supplement to medication in the case of rheumatoid arthritis, and should be sincerely considered for clinically diagnosed LOAD patients.

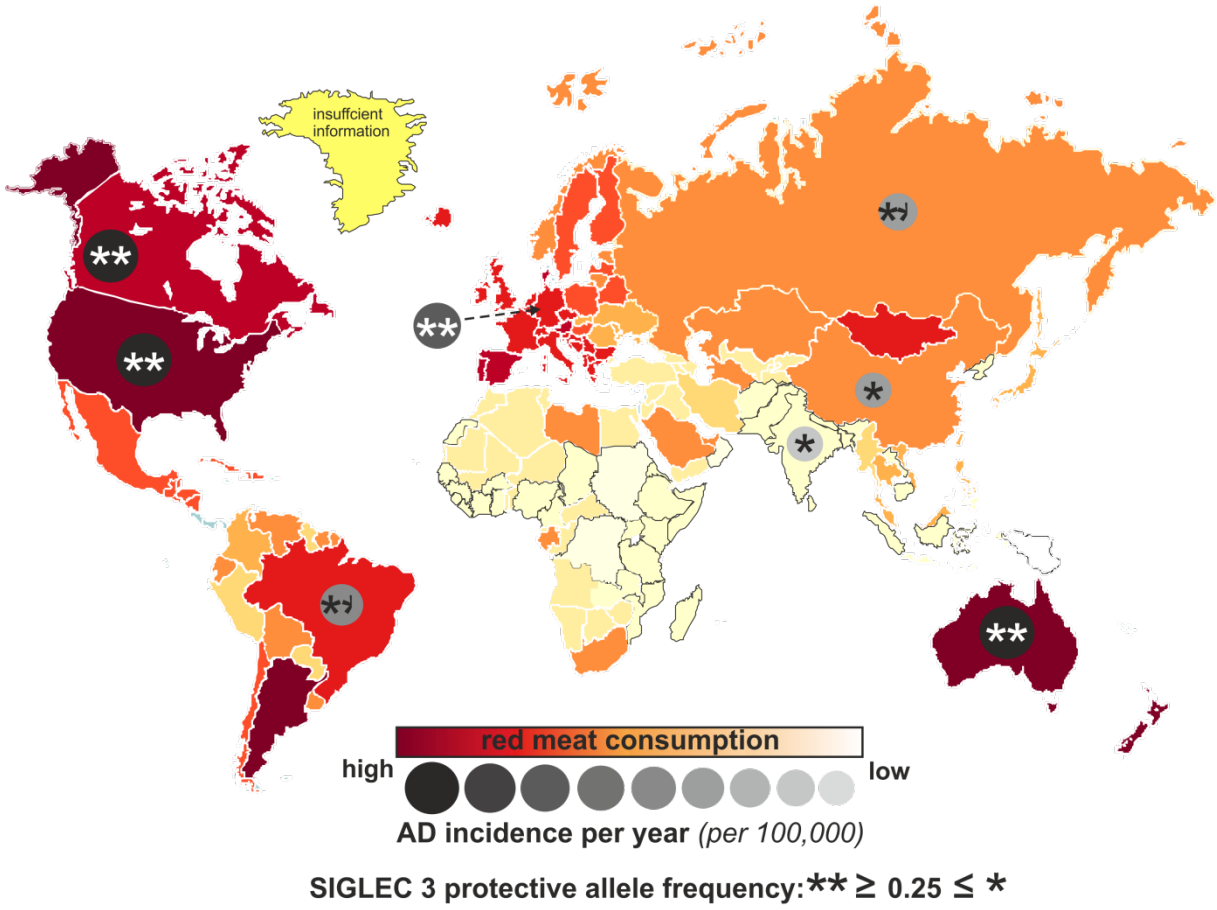

Figure 21: Global association between red meat consumption, AD risk and prevalence of SIGLEC3 protective allele. Epidemiological studies identified industrialized nations as the highest consumers and Asian and African continents as the lowest consumers of red meat. Research supported by the world health organization have identified the American and Australian continent as having the highest incidence of late onset Alzheimer's disease (LOAD), with Europe with a comparatively decreased incidence and Asian and African continents with the lowest incidence. Studies in the field of LOAD have identified highest prevalence of SIGLEC3 protective allele in Caucasian populations, followed by East-Asians and finally Africans and South-East Asians. Sources: blank world map: *https://www.printableworldmap.net/*. Modified to represent data on red meat consumption: protective allele frequency data: (Schwarz, Springer, et al. 2015)

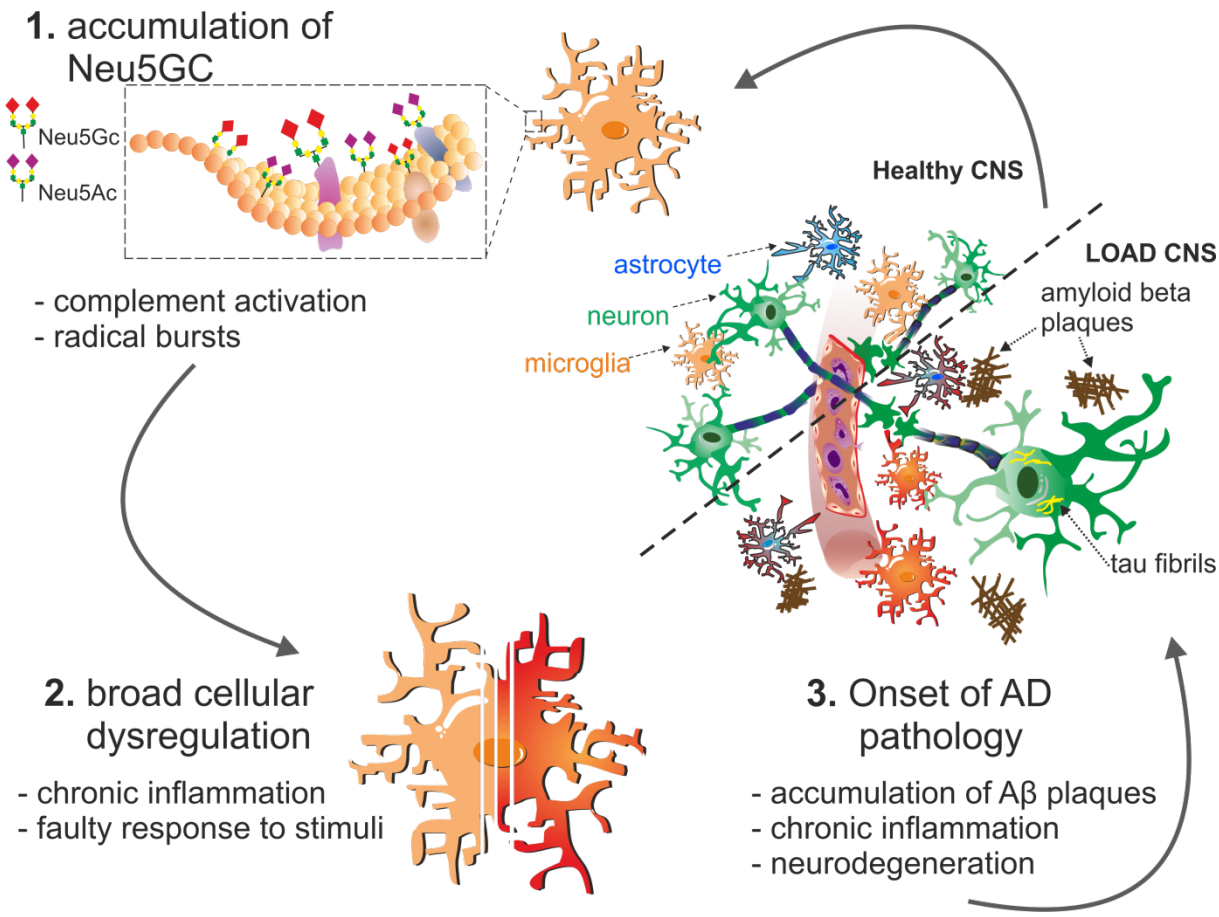

Figure 22: Neu5Gc induced microglial malfunctioning causes inflammation and can exacerbate LOAD pathology. Incorporation of Neu5Gc over time leads to an accumulation of this sialic acid. Accumulated sialic acid activates the complement cascade and causes radical bursts in the form of reactive oxygen species. Chronically inflammatory microglia forgo their responses to stimuli and fail to clear away deposited amyloid beta (Aβ). Left unchecked, Aβ accumulates into plaques which further activate surrounding glial cells. A vicious cycle of activation, inflammation and finally neurodegeneration develops.

5. Summary

Neuroinflammation and complement activation is believed to occur decades before clinical diagnosis of late onset Alzheimer's disease (LOAD). This project aimed to clarify the molecular environment that might modulate microglial activation prior to clinical diagnosis of LOAD. A human model system was used to study the human species-specific receptor sialic acid binding immunoglobulin-type lectin 3 (SIGLEC3) that has been associated with LOAD. SIGLEC3 can bind acetylated as well as glycosylated sialic acid (Neu5Ac and Neu5Gc, respectively). Neu5Gc cannot be produced by humans, but is metabolically incorporated in human cells after consumption of red meat or dairy products. Neu5Gc is known to cause xenosialitis, which involves an immune reaction in response to Neu5Gc incorporation.

First, human microglial cells (iPSdM9) were successfully differentiated from induced pluripotent stem (iPS) cells as a potential human model system to study SIGLEC3. Data indicate that the iPSdM9 microglial cells are capable of phagocytosis and proliferation. Furthermore, iPSdM9 cells positively express typical surface markers, namely IBA-1, TREM2 and CD11b. However, the limited cell numbers obtained hindered their use as a model system for molecular studies. For this reason, THP1 monocyte-derived macrophages were used as a surrogate human model system to study the role of SIGLEC3.

Effective incorporation of Neu5Gc into the THP1 macrophages by medium supplementation was confirmed by flow cytometry and xCGE-LIF analysis. RNA sequencing analysis established that incorporated Neu5Gc caused broad cellular dysregulation in comparison to cells cultured in Neu5Ac-supplemented medium, with more than 1400 differentially expressed genes. The particular pathways affected include cellular signaling, regulation of immune responses, immune cell development and responses to stimuli. While flow cytometry analysis using SIGLEC3 Fc-fusion proteins confirmed SIGLEC3 binding to Neu5Gc, western blot data determined that inhibitory signaling by SIGLEC3 was not effectively propagated. Therefore, Neu5Gc induced disruption of homeostatic SIGLEC3 signaling was hypothesized to cause malfunctioning of immune cells.

THP1 macrophages cultured in Neu5Ac-supplemented medium responded to Aβ treatment by increasing phagocytosis in a non-inflammatory manner. However, the

cells cultured in Neu5Gc-supplemented medium constitutively exhibited higher phagocytosis, accompanied by reactive oxygen species production. Furthermore, Aβ treatment of these cells did not increase phagocytosis, hinting at the dysfunctional immune response of cells carrying incorporated Neu5Gc. Additionally, real-time PCR analysis of classical complement cascade components revealed increased transcription of the complement components - c1q and c3, in cells cultured in Neu5Gc-supplemented medium. Taken together, Neu5Gc culture causes constitutive activation of macrophages. Interestingly, knocking out SIGLEC3 attenuates the Neu5Gc induced inflammatory characteristics but maintains increased phagocytosis upon Aβ treatment.

In conclusion, food-derived Neu5Gc is a possible candidate as an initiator for pre-clinical microglial dysfunction. Neu5Gc disrupts microglial immune responses and chronically induces radical production. Knocking out SIGLEC3 attenuates Neu5Gc induced inflammation and provides a possible therapeutic target against LOAD onset.

6. References

Abi-Rached, L. et al., 2011. The Shaping of Modern Human Immune Systems by Multiregional Admixture with Archaic Humans. *Science*, 334(6052), pp.89–94.

Angata, T., 2014. Associations of genetic polymorphisms of Siglecs with human diseases. *Glycobiology*, 24(9), pp.785–793.

Bardor, M. et al., 2005. Mechanism of uptake and incorporation of the non-human sialic acid N-glycolylneuraminic acid into human cells. *Journal of Biological Chemistry*, 280(6), pp.4228–4237.

Bergfeld, A.K. et al., 2012. Metabolism of vertebrate amino sugars with N-glycolyl groups: Elucidating the intracellular fate of the non-human sialic acid N-glycolylneuraminic acid. *Journal of Biological Chemistry*, 287(34), pp.28865–28881.

Beutner, C. et al., 2010. Generation of microglial cells from mouse embryonic stem cells. *Nature protocols*, 5(9), pp.1481–1494. Available at: http://dx.doi.org/10.1038/nprot.2010.90.

Bilimoria, P.M. & Stevens, B., 2015. Microglia function during brain development: New insights from animal models. *Brain Research*, 1617, pp.7–17.

Blix, F.G., Svennerholm, L. & Werner, I., 1952. The isolation of chondrosamine from gangliosides and from submaxillary mucin. *Acta Chem. Scand.*, 6, pp.358–362. Available at: http://actachemscand.dk/pdf/acta_vol_06_p0358-0362.pdf.

Blixt, O. et al., 2003. Sialoside specificity of the siglec family assessed using novel multivalent probes: Identification of potent inhibitors of myelin-associated glycoprotein. *Journal of Biological Chemistry*, 278(33), pp.31007–31019.

Bodea, L.-G. et al., 2014. Neurodegeneration by Activation of the Microglial Complement-Phagosome Pathway. *Journal of Neuroscience*, 34(25), pp.8546–8556. Available at: http://www.ncbi.nlm.nih.gov/pubmed/24948809%5Cnhttp://www.jneurosci.org/cgi/doi/10.1523/JNEUROSCI.5002-13.2014.

Bosurgi, L., Manfredi, A. a & Rovere-Querini, P., 2011. Macrophages in injured skeletal muscle: a perpetuum mobile causing and limiting fibrosis, prompting or restricting resolution and regeneration. *Frontiers in immunology*, 2(November),

p.62.

Bradshaw, E.M. et al., 2013. CD33 Alzheimer's disease locus: altered monocyte function and amyloid biology. *Nature Neuroscience*, 16(7), pp.848–850. Available at: http://www.nature.com/neuro/journal/v16/n7/full/nn.3435.html.

Brown, G.C. & Neher, J.J., 2014. Microglial phagocytosis of live neurons. *Nature Publishing Group*, 15(4), pp.209–216. Available at: http://dx.doi.org/10.1038/nrn3710%5Cnpapers2://publication/doi/10.1038/nrn3710.

Chan, G. et al., 2015a. CD33 modulates TREM2: convergence of Alzheimer loci. *Nature Neuroscience*, 18(11), pp.1556–1558. Available at: http://www.nature.com/neuro/journal/v18/n11/full/nn.4126.html%5Cnhttp://www.nature.com/neuro/journal/v18/n11/pdf/nn.4126.pdf.

Chan, G. et al., 2015b. CD33 modulates TREM2: convergence of Alzheimer loci. *Nature Neuroscience*, 18(11), pp.1556–1558. Available at: http://www.nature.com/neuro/journal/v18/n11/full/nn.4126.html%5Cnhttp://www.nature.com/neuro/journal/v18/n11/pdf/nn.4126.pdf.

Chin, J., 2011. Selecting a Mouse Model of Alzheimer's Disease. In E. D. Roberson, ed. *Alzheimer's Disease and Frontotemporal Dementia: Methods and Protocols*. Totowa, NJ: Humana Press, pp. 169–189. Available at: http://dx.doi.org/10.1007/978-1-60761-744-0_13.

Chou, H.-H. et al., 1998. A mutation in human CMP-sialic acid hydroxylase occurred after the Homo-Pan divergence. *Proceedings of the National Academy of Sciences of the United States of America*, 95(20), pp.11751–11756.

Claude, J. et al., 2013. Microglial CD33-related Siglec-E inhibits neurotoxicity by preventing the phagocytosis-associated oxidative burst. *The Journal of neuroscience : the official journal of the Society for Neuroscience*, 33(46), pp.18270–6. Available at: http://www.pubmedcentral.nih.gov/articlerender.fcgi?artid=3828472&tool=pmcentrez&rendertype=abstract.

Collins, B.E. et al., 1997. Products : Sialic Acid Specificity of Myelin-associated Glycoprotein Binding Sialic Acid Specificity of Myelin-associated Glycoprotein Binding *.

Colonna, M. & Wang, Y., 2016. TREM2 variants: new keys to decipher Alzheimer disease pathogenesis. *Nature Reviews. Neuroscience*, 17(4), pp.201–7. Available at: http://www.nature.com/doifinder/10.1038/nrn.2016.7%5Cnhttp://www.ncbi.nlm.nih.gov/pubmed/26911435.

Cooper, J.K. et al., 2007. Species identification in cell culture: a two-pronged molecular approach. *In vitro cellular & developmental biology. Animal*, 43, pp.344–351.

Coria, F. et al., 1993. The cellular pathology associated with Alzheimer β-amyloid deposits in non-demented aged individuals. *Neuropathology and Applied Neurobiology*, 19(3), pp.261–268. Available at: http://dx.doi.org/10.1111/j.1365-2990.1993.tb00436.x.

Crocker, P.R., Paulson, J.C. & Varki, A., 2007. Siglecs and their roles in the immune system. *Nat Rev Immunol*, 7(4), pp.255–266. Available at: http://dx.doi.org/10.1038/nri2056.

Davies, L.R.L. et al., 2012. Metabolism of vertebrate amino sugars with N-glycolyl groups: Resistance of ??2-8-linked N-glycolylneuraminic acid to enzymatic cleavage. *Journal of Biological Chemistry*, 287(34), pp.28917–28931.

Doens, D. et al., 2014. Microglia receptors and their implications in the response to amyloid β for Alzheimer's disease pathogenesis. *Journal of Neuroinflammation*, 11(1), p.48. Available at: http://jneuroinflammation.biomedcentral.com/articles/10.1186/1742-2094-11-48.

Doxey, A.C. & McConkey, B.J., 2013. Prediction of molecular mimicry candidates in human pathogenic bacteria. *Virulence*, 4(6), pp.453–66. Available at: http://www.ncbi.nlm.nih.gov/pubmed/23715053.

Edison, P. et al., 2008. Microglia, amyloid, and cognition in Alzheimer's disease: An [11C](R)PK11195-PET and [11C]PIB-PET study. *Neurobiology of disease*, 32(3), pp.412–9.

Eleftheriou, P. et al., 2014. Prevalence of anti-Neu5Gc antibodies in patients with hypothyroidism. *BioMed Research International*, 2014.

Esparza, T.J. et al., 2014. NIH Public Access. *Pathology*, 73(1), pp.104–119.

Fujita, P.A. et al., 2011. The UCSC genome browser database: Update 2011. *Nucleic*

Acids Research, 39(SUPPL. 1), pp.876–882.

Ginhoux, F. et al., 2010. Fate mapping analysis reveals that adult microglia derive from primitive macrophages. *Science (New York, N.Y.)*, 330(6005), pp.841–5.

Graham, L.C. et al., 2016. Chronic consumption of a western diet induces robust glial activation in aging mice and in a mouse model of Alzheimer's disease. *Scientific reports*, 6(February), p.21568. Available at: http://www.nature.com/srep/2016/160218/srep21568/full/srep21568.html.

Griciuc, A. et al., 2013. Alzheimer's disease risk gene cd33 inhibits microglial uptake of amyloid beta. *Neuron*, 78(4), pp.631–643. Available at: http://dx.doi.org/10.1016/j.neuron.2013.04.014.

Guerreiro, R. et al., 2013. TREM-2 variants in AD. , 368(2), pp.117–127.

Hedlund, M. et al., 2007. N-glycolylneuraminic acid deficiency in mice: implications for human biology and evolution. *Molecular and Cellular Biology*, 27(12), pp.4340–4346. Available at: http://www.ncbi.nlm.nih.gov/entrez/query.fcgi?cmd=Retrieve&db=PubMed&dopt=Citation&list_uids=17420276.

Hellwig, S. et al., 2015. Forebrain microglia from wild-type but not adult 5xFAD mice prevent amyloid-β plaque formation in organotypic hippocampal slice cultures. *Scientific reports*, 5(April), p.14624. Available at: http://www.pubmedcentral.nih.gov/articlerender.fcgi?artid=4586757&tool=pmcentrez&rendertype=abstract.

Heppner, F.L., Ransohoff, R.M. & Becher, B., 2015. Immune attack: the role of inflammation in Alzheimer disease. *Nat Rev Neurosci*, 16(6), pp.358–372. Available at: http://dx.doi.org/10.1038/nrn3880.

Herber, D.L. et al., 2007. Microglial Activation is Required for A$β$ Clearance After Intracranial Injection of Lipopolysaccharide in APP Transgenic Mice. *Journal of Neuroimmune Pharmacology*, 2(2), pp.222–231. Available at: http://dx.doi.org/10.1007/s11481-007-9069-z.

Hernández-Caselles, T. et al., 2006. A study of CD33 (SIGLEC-3) antigen expression and function on activated human T and NK cells: two isoforms of CD33 are generated by alternative splicing. *Journal of Leukocyte Biology* , 79(1), pp.46–58. Available at: http://www.jleukbio.org/content/79/1/46.abstract.

Hollingworth, P. et al., 2011. Europe PMC Funders Group Europe PMC Funders Author Manuscripts Europe PMC Funders Author Manuscripts Common variants in ABCA7 , MS4A6A / MS4A4E , EPHA1 , CD33 and CD2AP are associated with Alzheimer ' s disease. , 43(5), pp.429–435.

Hong, S. et al., 2016. Complement and microglia mediate early synapse loss in Alzheimer mouse models. *Science (New York, N.Y.)*, 352(6286), pp.712–6. Available at: http://www.ncbi.nlm.nih.gov/pubmed/27033548.

Johnson, D.J. et al., 2013. Shp1 regulates T cell homeostasis by limiting IL-4 signals. *The Journal of experimental medicine*, 210(7), pp.1419–31. Available at: http://www.ncbi.nlm.nih.gov/pubmed/23797092.

Kettenmann, H. et al., 2011. Physiology of Microglia. *Physiological Reviews*, 91(2), p.461 LP-553. Available at: http://physrev.physiology.org/content/91/2/461.abstract.

Kreutzberg, G.W., 1996. Microglia: a sensor for pathological events in the CNS. *Trends in neurosciences*, 19(8), pp.312–8.

Langmead, B. et al., 2009. 2C- Ultrafast and memory-efficient alignment of short DNA sequences to the human genome. *Genome Biol.*, 10(3), p.R25.

Lin, G.G. & Scott, J.G., 2012. NIH Public Access. , 100(2), pp.130–134.

Linnartz-Gerlach, B., Mathews, M. & Neumann, H., 2014. Sensing the neuronal glycocalyx by glial sialic acid binding immunoglobulin-like lectins. *Neuroscience*, 275.

Linnartz, B., Wang, Y. & Neumann, H., 2010. Microglial immunoreceptor tyrosine-based activation and inhibition motif signaling in neuroinflammation. *International journal of Alzheimer's disease*, 2010.

Lull, M.E. & Block, M.L., 2011. NIH Public Access. *October*, 7(4), pp.354–365.

Ma, F. et al., 2016. A Mouse Model for Dietary Xenosialitis: ANTIBODIES TO XENOGLYCAN CAN REDUCE FERTILITY. *The Journal of biological chemistry*, 291(35), pp.18222–31. Available at: http://www.jbc.org/cgi/content/long/M116.739169v1 [Accessed October 28, 2016].

Maderna, P. & Godson, C., 2003. Phagocytosis of apoptotic cells and the resolution

of inflammation. *Biochimica et Biophysica Acta - Molecular Basis of Disease*, 1639(3), pp.141–151.

Malik, M. et al., 2013. CD33 Alzheimer's risk-altering polymorphism, CD33 expression, and exon 2 splicing. *The Journal of neuroscience : the official journal of the Society for Neuroscience*, 33(33), pp.13320–5. Available at: http://www.pubmedcentral.nih.gov/articlerender.fcgi?artid=3742922&tool=pmcentrez&rendertype=abstract.

Malik, M. et al., 2015. Genetics ignite focus on microglial inflammation in Alzheimer's disease. *Molecular Neurodegeneration*, 10(1), p.52. Available at: http://www.pubmedcentral.nih.gov/articlerender.fcgi?artid=4595327&tool=pmcentrez&rendertype=abstract.

Malykh, Y.N., Schauer, R. & Shaw, L., 2001. N-Glycolylneuraminic acid in human tumours. *Biochimie*, 83(7), pp.623–634.

Mayshar, Y. et al., 2010. Identification and Classification of Chromosomal Aberrations in Human Induced Pluripotent Stem Cells. *Stem Cell*, 7(4), pp.521–531. Available at: http://dx.doi.org/10.1016/j.stem.2010.07.017%5Cnpapers2://publication/doi/10.1016/j.stem.2010.07.017.

Mclaurin, J. & Ransohoff, R., 2010. com mu n i t y co r n e r Microglial pilgrimage to the brain. , 152(1999), pp.1380–1381.

Michelucci, A. et al., 2009. Characterization of the microglial phenotype under specific pro-inflammatory and anti-inflammatory conditions: Effects of oligomeric and fibrillar amyloid-?? *Journal of Neuroimmunology*, 210(1–2), pp.3–12.

Milton, R.H. et al., 2008. CLIC1 Function Is Required for -Amyloid-Induced Generation of Reactive Oxygen Species by Microglia. *Journal of Neuroscience*, 28(45), pp.11488–11499. Available at: http://www.jneurosci.org/cgi/doi/10.1523/JNEUROSCI.2431-08.2008.

Naj, A.C. et al., 2011. Common variants in MS4A4/MS4A6E, CD2uAP, CD33, and EPHA1 are associated with late-onset Alzheimer's disease Adam. *Nature genetics*, 43(5), pp.436–441.

Nimmerjahn, A., Kirchhoff, F. & Helmchen, F., 2005. Resting microglial cells are highly dynamic surveillants of brain parenchyma in vivo. *Science (New York,*

N.Y.), 308(5726), pp.1314–8.

Noonan, J.P., 2010. Neanderthal genomics and the evolution of modern humans Neanderthal genomics and the evolution of modern humans. *Genome*, 20, pp.547–553.

Padler-Karavani, V., Tremoulet, A.H., et al., 2013. A Simple Method for Assessment of Human Anti-Neu5Gc Antibodies Applied to Kawasaki Disease. *PLoS ONE*, 8(3).

Padler-Karavani, V. et al., 2014. Rapid evolution of binding specificities and expression patterns of inhibitory CD33-related Siglecs in primates. *FASEB Journal*, 28(3), pp.1280–1293.

Padler-Karavani, V., Hurtado-Ziola, N., et al., 2013. Rapid evolution of binding specificities and expression patterns of inhibitory CD33-related Siglecs in primates. *FASEB journal : official publication of the Federation of American Societies for Experimental Biology*, pp.1–14.

Paolicelli, R.C. et al., 2011. Synaptic Pruning by Microglia Is Necessary for Normal Brain Development. *Science*, 333(6048), p.1456 LP-1458. Available at: http://science.sciencemag.org/content/333/6048/1456.abstract.

Parajuli, B. et al., 2013. Oligomeric amyloid β induces IL-1β processing via production of ROS: implication in Alzheimer's disease. *Cell death & disease*, 4, p.e975. Available at: http://www.pubmedcentral.nih.gov/articlerender.fcgi?artid=3877570&tool=pmcentrez&rendertype=abstract.

Rachmilewitz, J., 2010. Glycosylation: an intrinsic sign of "Danger." *Self/Nonself*, 1(3), pp.250–254.

Ransohoff, R.M. & Cardona, A.E., 2010. The myeloid cells of the central nervous system parenchyma. *Nature*, 468(7321), pp.253–62.

Ridolfi, E. et al., 2013. The Role of the Innate Immune System in Alzheimer's Disease and Frontotemporal Lobar Degeneration: An Eye on Microglia. *Clinical and Developmental Immunology*, 2013, p.10.1155/2013/939786.

Roy, K., 2012. Establishment of microglial precursors derived from human induced pluripotent stem cells to model SOD1-mediated amyotrophic lateral sclerosis. , (August).

Samraj, A.N. et al., 2015. A red meat-derived glycan promotes inflammation and cancer progression. *Proceedings of the National Academy of Sciences of the United States of America*, 112(2), pp.542–7. Available at: http://www.pubmedcentral.nih.gov/articlerender.fcgi?artid=4299224&tool=pmcentrez&rendertype=abstract.

Schnaar, R.L., Gerardy-Schahn, R. & Hildebrandt, H., 2014. Sialic acids in the brain: gangliosides and polysialic acid in nervous system development, stability, disease, and regeneration. *Physiological reviews*, 94, pp.461–518. Available at: http://www.ncbi.nlm.nih.gov/pubmed/24692354.

Schwarz, F., Springer, S.A., et al., 2015. Human-specific derived alleles of CD33 and other genes protect against postreproductive cognitive decline. *Proceedings of the National Academy of Sciences*, (April 2016), p.201517951. Available at: http://www.pnas.org/lookup/doi/10.1073/pnas.1517951112%5Cnpapers3://publication/doi/10.1073/pnas.1517951112.

Schwarz, F., Pearce, O.M.T., et al., 2015. Siglec receptors impact mammalian lifespan by modulating oxidative stress. *eLife*, 4, pp.1–19.

Shi, H. et al., 2012. Genetic variants influencing human aging from late-onset Alzheimer's disease (LOAD) genome-wide association studies (GWAS). *Neurobiology of Aging*, 33(8).

Solito, E. & Sastre, M., 2012. Microglia function in Alzheimer's disease. *Frontiers in pharmacology*, 3(February), p.14.

Streit, W.J., 2004. Microglia and Alzheimer's disease pathogenesis. *Journal of Neuroscience Research*, 77(1), pp.1–8.

Taguchi, R. et al., 2015. Preferential Accumulation of 14C-N-Glycolylneuraminic Acid over 14C-N-Acetylneuraminic Acid in the Rat Brain after Tail Vein Injection. *Plos One*, 10(6), p.e0131061. Available at: http://dx.plos.org/10.1371/journal.pone.0131061.

Tangvoranuntakul, P. et al., 2003. Human uptake and incorporation of an immunogenic nonhuman dietary sialic acid. *Proc Natl Acad Sci U S A*, 100(21), pp.12045–12050. Available at: http://www.ncbi.nlm.nih.gov/pmc/articles/PMC218710/pdf/10012045.pdf.

Tosto, G. & Reitz, C., 2013. Genome-wide association studies in Alzheimer's

disease: A review topical collection on dementia. *Current Neurology and Neuroscience Reports*, 13(10).

Trapnell, C. et al., 2012. Differential gene and transcript expression analysis of RNA-seq experiments with TopHat and Cufflinks. *Nat. Protocols*, 7(3), pp.562–578. Available at: http://dx.doi.org/10.1038/nprot.2012.016.

Trapnell, C. et al., 2010. Transcript assembly and quantification by RNA-Seq reveals unannotated transcripts and isoform switching during cell differentiation. *Nature Biotechnology*, 28(5), pp.511–515. Available at: http://www.nature.com/nbt/journal/v28/n5/full/nbt.1621.html%5Cnhttp://www.nature.com/nbt/journal/v28/n5/pdf/nbt.1621.pdf.

Trapnell, C., Pachter, L. & Salzberg, S.L., 2009. TopHat: Discovering splice junctions with RNA-Seq. *Bioinformatics*, 25(9), pp.1105–1111.

Tremblay, M.-È., Lowery, R.L. & Majewska, A.K., 2010. Microglial interactions with synapses are modulated by visual experience. *PLoS biology*, 8(11), p.e1000527.

Varela, C. et al., 2012. Reccurent genomic instability of chromosome 1q in neural derivatives of human embryonic stem cells. , 122(2), pp.2–7.

Varki, A., 2010. Colloquium paper: uniquely human evolution of sialic acid genetics and biology. *Proceedings of the National Academy of Sciences of the United States of America*, 107 Suppl, pp.8939–46.

Varki, A., 2007. Glycan-based interactions involving vertebrate sialic-acid-recognizing proteins. , 446(April), pp.1023–1029.

Varki, A., 2001. Loss of N-glycolylneuraminic acid in humans: Mechanisms, consequences, and implications for hominid evolution. *American journal of physical anthropology*, Suppl 33, pp.54–69.

Varki, A. & Gagneux, P., 2012. Multifarious roles of sialic acids in immunity. , 1253, pp.16–36.

Varnum, M.M. & Ikezu, T., 2012. The classification of microglial activation phenotypes on neurodegeneration and regeneration in alzheimer's disease brain. *Archivum Immunologiae et Therapiae Experimentalis*, 60(4), pp.251–266.

Wang, X. et al., 2012. Specific inactivation of two immunomodulatory SIGLEC genes during human evolution. *Proceedings of the National Academy of Sciences*,

109(25), pp.9935–9940.

Wang, Y. et al., 2015. TREM2 lipid sensing sustains the microglial response in an Alzheimer's disease model. *Cell*, 160(6), pp.1061–1071. Available at: http://dx.doi.org/10.1016/j.cell.2015.01.049.

Wu, Y. et al., 2016. Microglia: Dynamic Mediators of Synapse Development and Plasticity. *Trends in Immunology*, 36(10), pp.605–613. Available at: http://dx.doi.org/10.1016/j.it.2015.08.008.

Yeh, F.L. et al., 2016. TREM2 Binds to Apolipoproteins, Including APOE and CLU/APOJ, and Thereby Facilitates Uptake of Amyloid-Beta by Microglia. *Neuron*, 91(2), pp.328–40. Available at: http://linkinghub.elsevier.com/retrieve/pii/S0896627316302926%5Cnhttp://www.ncbi.nlm.nih.gov/pubmed/27477018.

Yokokura, M. et al., 2011. In vivo changes in microglial activation and amyloid deposits in brain regions with hypometabolism in Alzheimer's disease. *European Journal of Nuclear Medicine and Molecular Imaging*, 38(2), pp.343–351. Available at: http://dx.doi.org/10.1007/s00259-010-1612-0.

Acknowledgements / Danksagung

I would like to extend much gratitude towards Prof. Harald Neumann for accepting me as part of his research team and guiding me through this fascinating project. I appreciate every moment of success as well as failure with which came the opportunity to learn and grow. I would like to also thank my second supervisor, Prof. Walter Witke for his positive involvement and insights into my PhD project. I am very grateful to Dr. Heike Weighardt and Prof. Bovier, who both graciously accepted to execute their duties as third and fourth members of my examination committee.

Special thanks go out to all the members in the Institute of Reconstructive Neurobiology, especially the AG Neumann family. I enjoyed every moment of my time as part of the group both inside and outside of the lab. I will always appreciate the wonderful friendship of Rita Jietou, Jessica Reinartz, Janine Claude, Marcus Grobe-Einsler and Johannes Ackermann. I am grateful for the memories and support from Dr. Liviu Bodea and Dr. Gabriela Bodea, Dr. Anahita Shahraz, Dr. Bettina Linnartz-Gerlach, Dr. Jens Kopatz, Dr. Ichiro Nozaki, Christine Schuy, Ozkan Is, Omar Mossad, Sharon Stursburg, Sevgi Cengiz and many more.

Most importantly, I am ever grateful and appreciative of my supportive partner, Dr. Jesuthas Ajendra and his loving family. I extend my utmost gratitude, love and wishes to my own family to whom I owe every milestone that I have achieved so far. Especially, to my mother, Meena Mathews and sister Liza Mathews-Ram, thank you for supporting me every step of the way.

Declaration / Erklärung

I, Mona Ann Mathews, hereby confirm that this work submitted is my own. This thesis has been written independently, and with no other sources or aids than stated. The presented thesis has not been submitted to another university and I have not applied for a doctorate procedure so far.

Hiermit versichere ich, dass die vorgelegte Arbeit - abgesehen von den ausdrücklich bezeichneten Hilfsmitteln - persönlich, selbständig und ohne Benutzung anderer als der angegebenen Hilfsmittel angefertigt wurde. Aus anderen Quellen direkt oder indirekt übernommene Daten und Konzepte sind unter Angabe der Quelle kenntlich gemacht worden.
Die vorliegende Arbeit wurde an keiner anderen Hochschule als Dissertation eingereicht. Ich habe früher noch keinen Promotionsversuch unternommen.

Bonn, November 2016

Mona Ann Mathews